# IMPI's 51st Annual Microwave Power Symposium (IMPI 51)

# 2017 PROCEEDINGS

## June 20-22, 2017

**Sonesta Hotel, Coconut Grove**
**Miami, FL, USA**

ISSN 1070-0129

Presented by the
INTERNATIONAL MICROWAVE POWER INSTITUTE
PO Box 1140, Mechanicsville, VA 23111
Phone: +1 (804) 559 6667 • Email: info@impi.org
WWW.IMPI.ORG

# Welcome to Miami for the 51st IMPI Symposium

Each year, IMPI brings together researchers from across the globe to share the latest findings in microwave and RF heating theories and applications, and this year we have an outstanding array of researchers in attendance. If you are not yet a member of IMPI, we strongly encourage you to consider joining onsite. IMPI membership connects you to microwave and RF academia, researchers, developers and practitioners across the globe. Talk to an IMPI member today to learn more about the value of joining our outstanding organization!

Thank you for joining us. We hope you learn from the technical presentations, interact with your colleagues, and enjoy the atmosphere of the Symposium. And do take the opportunity to visit the many interesting sites in and around Miami.

Special thanks to the following partners for printing these Proceedings:

LIVERPOOL JOHN MOORES UNIVERSITY

BEST — Built Environment & Sustainable Technologies Research Institute

IMPI wishes to express its gratitude to the following individuals:

## TECHNICAL PROGRAM COMMITTEE

Graham Brodie, University of Melbourne, Australia
Ric Gonzalez, Conagra Brands, Inc., USA

Members
Vladimir Bilik, S-TEAM Lab, The Slovak Republic
Raymond Boxman, Tel Aviv University, Israel
Georgios Dimitrakis, University of Nottingham, UK
John F. Gerling, GAE, Inc., USA
Satoshi Horikoshi, Sophia University, Japan
Marilena Radoiu, Independent Consultant, France
Klaus Werner, RF Energy Alliance, The Netherlands
Roger Williams, AMPLEON, USA
Vadim V. Yakovlev, Worcester Polytechnic Institute, USA

## FOOD SCIENCE AND TECHNOLOGY COMMITTEE

Bob Schiffmann, R.F. Schiffmann Associates Inc., USA

Members
Gordon Andrews, Gama Consulting, UK
John Bows, Pepsico, United Kingdom
Sumeet Dhawan, Nestle R & D, USA
Ulrich Erle, Nestle R & D, USA
Marie Jirsa, Tyson Foods, USA
Nigel McCulloch, Cucina Sano, Italy
Jeyamkondan Subbiah, University of Nebraska- Lincoln, USA
Juming Tang, Washington State University, USA
Mark Watts, Campbell Soup Company, USA

*Purchasing Information: Copies of the Proceedings of the 51st Annual Microwave Power Symposium, as well as back issues from prior years, are available for purchase. Contact Molly Poisant, Executive Director of IMPI, at +1 804 559 6667 or molly.poisant@impi.org for details.*

# Table of Contents

## Solid State Spotlight



## Materials Processing & Applicator Design



## Food & Agriculture and Food Processing I

# Table of Contents

# Table of Contents

## FOOD SAFETY & STANDARDS

# Notes

# Solid-state RF Energy: Applicator and Software Considerations for Industrial Applications

**Dr. Klaus Werner**

RF Energy Alliance, Beaverton, Oregon 97003 USA
www.rfenergy.org

**Keywords**: Solid state RF power amplifiers, RF energy applications, industrial applications, software, applicator, RF Energy Alliance

**SHORT ABSTRACT**

Solid-state radio frequency (RF) technology used for heating and power delivery applications has taken hold in the last couple of years in a number of markets and has given rise to the notion of RF Energy applications. Examples of solid-state RF Energy applications can be found in consumer microwave ovens, RF plasma lighting, automotive plasma ignition, medical cancer treatments, and many others. Most noteworthy, are all kinds of industrial heating, drying, curing, sintering or similar processes that are currently being developed with solid-state RF rather than the legacy magnetron as the driving source.

My presentation at IMPI 2016, "Recognizing design challenges of solid-state power amplifiers for RF energy applications," discussed various technical challenges associated with the design of solid-state RF energy systems and the work being done to address those concerns. As a follow up in the series, this paper will focus on the systems level and application specific requirements for industrial RF Energy use cases.

Specifically, the presentation will cover a number of system engineering design choices for the applicator, that is the very "cavity" or "space" where the interactions of the microwaves with matter take place, for a variety of industrial RF Energy applications, including cooking, lighting, and plasma jets. I will also demonstrate how the same basic RF Energy hardware architecture can drive all of these applications with adaptions in control software and actual power level as necessary for specific applicators/applications. Furthermore, the paper will highlight the recent RF Energy Alliance progress in developing specifications and guidelines for the advancement of industrial RF Energy applications.

# A New RF Thawing System Based on LDMOS

**Junhong Li**

Wattsine Electronic Technology Co., Ltd, Chengdu, China

**Keywords:** RF, thawing, solid-state, LDMOS.

## INTRODUCTION

The purpose of freezing food is to keep the freshness and the storage time of the food as much as possible. Thus, all the refrigerator companies in the world spared no efforts to develop food freezing and fresh keeping equipment with ranges of functions.

As the reverse process of freezing, thawing was always ignored during the application of food. Inappropriate ways of thawing is applied only to make the food which have been perfectly frozen destroyed. The surface of the food will be deteriorated and polluted with nutrition loss. The existing thawing methods such as naturally thawing, cold-water thawing and microwave-oven thawing will face this situation for a long time.

Wattsine has developed a new thawing system based on a solid-state RF generator which overcomes many of the problems with thawing in a conventional microwave oven.

## METHODOLOY

Our thawing equipment is a cavity working at a frequency of 433 MHz, adopting a parallel plate antenna as the energy radiator, radiating microwave energy to the thawing cavity. 433Mhz band is a balanced choice considering of efficiency and microwave penetration. In fact, we do start with 13.56Mhz and have found some cost disadvantages and engineering difficulties during the system integration:

- Cost disadvantages (i.e. matcher and capacitance cost)
- Power consumption disadvantages (compared with 433Mhz)
- System instability (disrupted by external interference)
- Much more modulation effort required (compared with 433Mhz)

The width of the cavity is 28cm, which is shorter than the half-wave length of the working frequency. When the cavity is empty, the equipment will be cut-off. When the cavity is loaded, the microwave energy will be absorbed by the load.

The thawing system includes an AC-DC power supplier, the 433 MHz solid-state power generator. The microprocessor controls the working condition of the 433 MHz solid-state generator according to the operation of the Human Machine Interaction and heating algorithm. The RF power out of the system is 200W. The applied solid-state power generator is composed with signal generator, control processor, power supply, power driver, gain control, main power amplifier, circulator and positive/reverse power detection circuit. The total energy consumption of the thawing system is less than 280w.

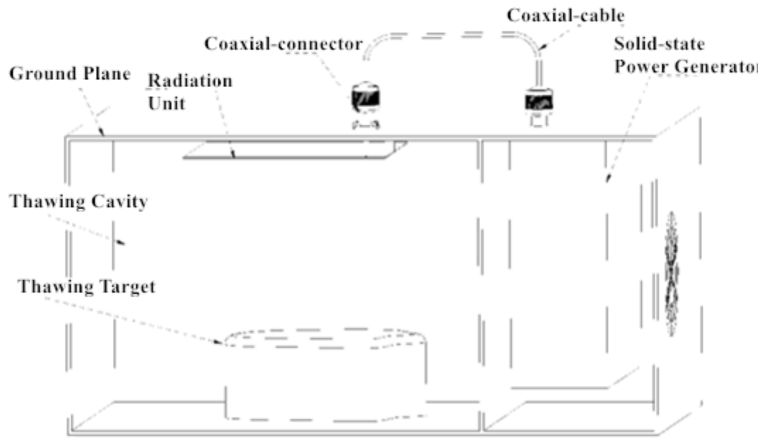


Figure 1. Schematic diagram of the solid-state RF thawing system developed by Wattsine

## RESULTS

We prepared 3 pieces of pork weighing about 500g with irregular shapes. Thawed them with naturally, microwave-oven and solid-state RF equipment for 10 minutes, then directly observing with naked eyes:

| Naturally thawing | Microwave-oven thawing (2.45GHz) | Solid-state RF thawing |
|---|---|---|
| No significant effect of thawing. | Thawed with deterioration on the surface and blood flow. | Well thawed with intact surface an no blood flow. |
|  | 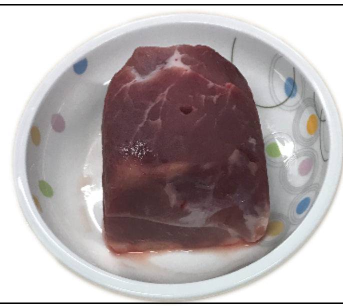 |  |

Figure 2. Thawing effect of 3 different methods of thawing

**RF delivery chain comparison**

| | efficiencies | | | |
|---|---|---|---|---|
| | Magnetron | | SSC | |
| subsystem | typical | ECI test | LDMOS | GaN |
| AC -> DC | 85% | 90% | 93% | 93% |
| RF generation | 60% | 70% | 50% | 70% |
| RF cabling | 95% | 95% | 95% | 95% |
| Antennae | 95% | 95% | 90% | 90% |
| cavity | 95% | 95% | 95% | 95% |
| RF to food coupling | 40% | 90% | 93% | 93% |
| | | | | |
| **wall plug efficiency:** | **17%** | **49%** | **35%** | **49%** |

Figure 3. RF delivery chain comparison between magnetron and solid-state semiconductor

| Ingredient | Initial Temperature | Ending Temperature | Thawing Time | Cutting Degree |
|---|---|---|---|---|
| Lean pork 250g | -17.6 | -4 | 8 minutes | Very easy to cut |
| Lean prok 500g | -18.8 | -4.8 | 10 minutes | Easy to cut |
| Beef 250g | -17.3 | -4 | 9 minutes | Very easy to cut |
| Beef 500g | -18.4 | -4.7 | 12 minutes | Easy to cut |

Figure 4. The RF thawing system tested with different weight and different types of commonly used food.

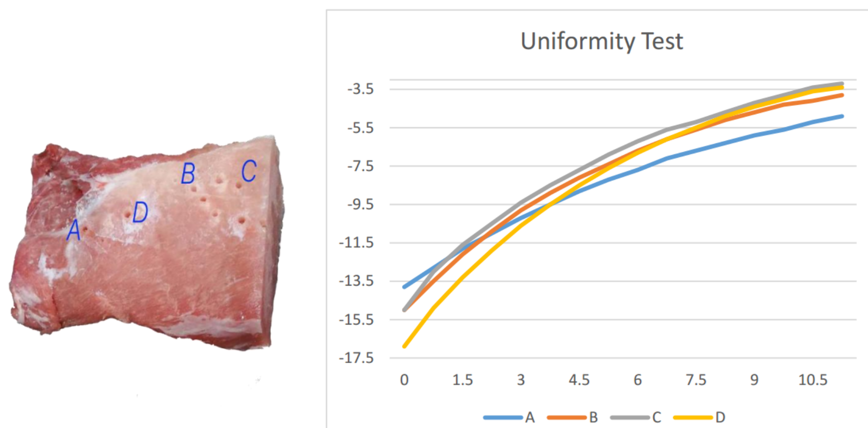


Figure 5. Excellent homogeneity showed in the test of the RF thawing system

## DISCUSSION

The solid-state RF thawing system can penetrate deeper to the target. With the parallel plate antenna and special cavity structure of the system, the target will be thawed more homogeneously. The system can automatically search for the best resonant frequency according to the characteristic of targeted food. The system also can transform between electronic and microwave energy efficiently. Further more, safety is guaranteed because it can automatically sweep VSWR, and is equipped with built-in control tracking, monitoring and protection circuit. It will automatically cut-off when it’s empty-loaded or thawed overturned. Thawing time can be accurately set within 1- 15 minutes. Meanwhile, the new solid-state RF thawing system can be easily controlled with real-time feedback and adjustment of operating frequency, phase, and power (forward & reverse). The compact structure and modular design of the system is available for easier system expansion and maintenance.

Compared to the traditional thawing methods, the new system showed a better performance in thawing time, thawing homogeneity and thawing effect.

## CONCLUSION

The new thawing system based on solid-state RF generator can thaw your food to perfection. It will be a better choice for both home cooking and professional cooking.

# Compact 2.45 GHz Solid-state Plasma Sources for Industrial and Laboratory Applications

**K. Achkasov[1], L. Latrasse[1], M. Radoiu[1*], J. Lo[2] and P. Guillot[2]**

[1]SAIREM SAS, 12 Porte du Grand Lyon, Neyron 01700, France
[2]Plasma Diagnostic Research Team, CUFR Jean François Champollion, Place de Verdun, Albi 81012, France
e-mail: kachkasov@sairem.com

**Keywords**: microwave plasma, solid-state technology, electron-cyclotron resonance, collisional regime, Langmuir probe, surface wave.

## INTRODUCTION

Microwaves are frequently used to produce high density plasmas for industrial and laboratory applications. These sources present several advantages when compared to radio-frequency and DC discharges such as high reactive species density and no need for electrodes. Technological advances over the last few years calls for large-scale processing with high density and uniform plasma at reduced and atmospheric pressure.

To meet these industrial requirements **Aura-Wave** [1], an electron cyclotron resonance (ECR) coaxial microwave plasma source working in the $10^{-2}$ – 1 Pa pressure range and **Hi-Wave**, a collisional plasma source for higher pressure gas processing, i.e. 1 – 100 Pa have been designed. Each plasma source is powered by its own microwave solid state generator, so multiple sources operating in different conditions (gas type, pressure, MW power) can be distributed together in the same reactor. In this design the solid-state microwave generator can produce a forward wave with variable frequency (2400 MHz – 2500 MHz) which enables an automatic adjustment loop of the reflected power, created occasionally by a change in the operating conditions [2].

Atmospheric plasma sources are widely requested in applications such as surface functionalization, elementary analysis, creation of radicals and reactive species as well as a broad use in medicine (sterilization/disinfection, bacterial inactivation, treatment of chronic wounds, etc.). For these purposes, **S-Wave** (a compact plasma source named after "Surface Wave") has been developed. This plasma source can operate in the range of a few $10^{-2}$ mbar to atmospheric pressure and is able to create and maintain plasma columns with variable lengths. By positioning the substrate 20 – 30 cm downstream the **S-Wave**, surface

* At present this author is an independent consultant

treatment by reactive species is possible while avoiding the direct contact with the high temperature plasma column. An ignition system based on dielectric barrier discharge allows to breakdown easily even at atmospheric pressure. **S-Wave** operates optimally in connection with a low ripple 200 W microwave solid-state generator.

## METHODOLOGY

The coaxial antenna using the ECR to generate plasma (**Aura-Wave** in Figure 1a) consists of encapsulated cylindrical permanent magnets, mounted in opposition within the coaxial structure. This arrangement enables to generate a magnetic field in the direction of the center of the plasma chamber and hence, limiting losses on the walls. The source was designed to reach plasma densities up to a few $10^{11}$ $cm^{-3}$ in multisource configuration (Fig. 1b) at 10 cm from the source. The coaxial antenna based on collisional heating called (**Hi-Wave** in Figure 1c) was designed to reach plasma densities of $10^{11}$-$10^{12}$ $cm^{-3}$ at 10 cm from the source, depending on the gas, in multisource configuration (Figure 1d).

The **S-Wave** plasma source (shown in Figure 1e) is inductively coupled, thus only two tuning adjustments are provided to match the impedance. Generally, nearly 0 % of reflected power is achieved using the integrated tuners. The plasma is created in a dielectric tube placed inside the source; the external diameter of the tube is either 6 mm or 8 mm. The microwave electric field propagates longitudinally at the dielectric/plasma interface, i.e. plasma behaves as an electrical conductor; radially the wave is strongly attenuated at skin depth. This principle allows to create and maintain plasma columns with lengths that depend on the operating pressure, microwave power and gas type. For given operator-set discharge conditions, the plasma is fully reproducible without any need for retuning at start-up. Quick connectors are integrated for water cooling and for inlet gas connection.

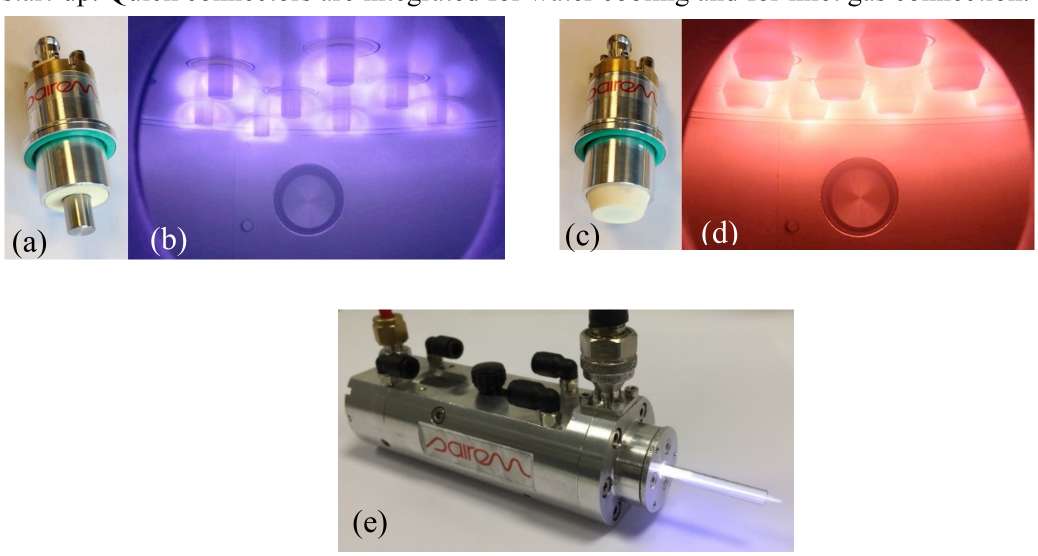


Figure 1. (a) *Aura-Wave* ECR microwave plasma source. (b) Multisource reactor consisting of 8 *Aura-Wave* units (shown in argon for a total microwave power of 160 W at 1 Pa). (c) *Hi-Wave* collisional microwave plasma source. (d) Multisource reactor consisting of 8 *Hi-Wave* units (shown in nitrogen for a total microwave power of 1600 W at 10 Pa). (e) Photo of the atmospheric plasma created by S-Wave (without ignition system). Argon, microwave power 200 W.

## RESULTS

Plasma parameters - plasma density, electron temperature and uniformity - were measured with a Langmuir probe placed at two heights, d = 85 mm and d = 160 mm from the plasma sources. In circular matrix, 8 off × Hi-Wave plasma sources were tested - see the source positioning in the inset of Figure 2(a). The diameter of the circular configuration is 247 mm; 200 W of microwave power supplied to each source, pressure 5 Pa. The plasma density profiles are plotted in Figure 2 for $O_2$. Plasma uniformity of 1.65 % at d = 85 mm and 1.8 % at d = 160 mm over 250 mm area diameter was measured. The Optical Emission Spectroscopy measurements were performed to see the dependence of reactive species line emission on the forward power which has proven to be linear, as shown in Figure 3(b).

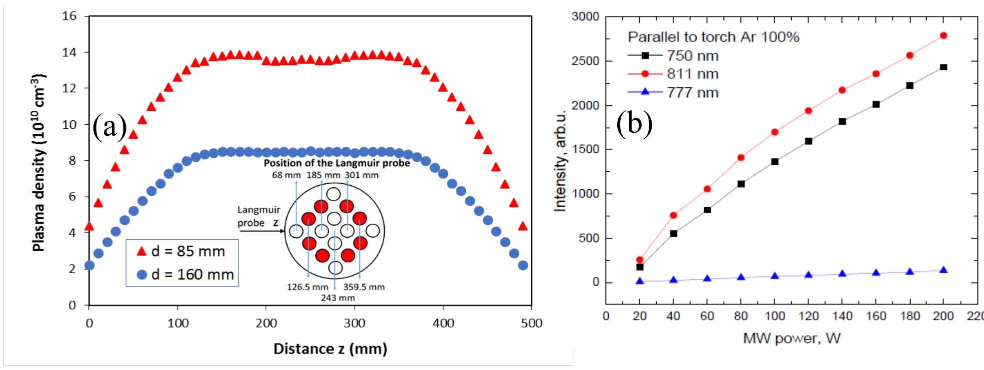


Figure 2. (a) Oxygen plasma distribution uniformity vs. distance and diameter at d = 85 mm and d = 160 mm from the Hi-wave sources. (b) Evolution of Ar and $O_2$ emission lines as a function of MW power measured in pure Ar plasma. Fiber orientation: parallel to the torch.

## CONCLUSION

**Aura-Wave** and **Hi-Wave** – plasma sources operating at reduced pressure - allow to produce large, uniform and high density plasma without scale limitation and equally, to reach uniform plasma over large treatment areas. Both sources are self-adapted on a wide range of operating conditions. **S-Wave,** compact plasma torch with incorporated DBD ignition system, demonstrated reproducible thermal plasmas at reduced and atmospheric pressures being a well suited plasma sources for production of reactive species, sterilization, bacterial inactivation, etc.

## REFERENCES

[1] S. Béchu, A. Bès, A. Lacoste, J. Pelletier, Device and method for producing and/or confining a plasma, *Patent WO 2010049456*.

[2] L. Latrasse, M. Radoiu, J.-M. Jacomino, A. Grandemenge, Facility for microwave treatment of a load, *Patent WO 2012146870*.

# New RF Connectivity Concepts for RF-energy Applications in Mass Manufacturing

**Hannes Grubinger, Michael Rupflin, Martin Wagner, Ulf Hügel**

HUBER+SUHNER AG, 9100 Herisau, Switzerland

**Keywords**: RF connectivity, RF solid state amplifier, RF energy.

## INTRODUCTION

Using solid-state generated and amplified RF-power [1] for applications including cooking and warming brings a completely new user experience to the respective applications. This is mainly due to the better controllability of amplifiers, when compared to magnetrons. RF power amplifiers in RF-energy applications have a lot of similarities with amplifiers used in communication industries. The main differences however are the additional higher power levels and the focus on power use instead of signal quality and linearity.

Replacing magnetrons by solid state amplifiers has also a significant impact to the connectivity required in such an application. Magnetrons are optimized for coupling into a rectangular waveguide. Power amplifiers however will be realized on a printed circuit board calling for different concepts. Connectors [2] and cables as used in communication industry are often not the perfect solution, since losses and cost of coaxial assemblies may appear not appropriate for the short distances in kitchen appliances. Further, ambient temperature in the application is high which reduce the performance of cables additionally due to significant reduced power capability caused by the used dielectric materials [3]. The appliance assembly process calls for simple and fast processes which are not supported by threaded connector. Further, there are many requirements in communication industry (for example PIM = passive intermodulation) adding cost to components, which certainly are not adding value in energy applications.

## OPTIONS ADRESSING SPECIFIC ENERGY REQUIREMENTS

HUBER+SUHNER has worked on a couple of concepts which overcome most of the above mentioned disadvantages, but allow for a reliable and robust connection between amplifier and cooking cavity. The following examples are very much based on cooking applications, but can be easily adapted for other applications (such as lighting, microwave ablation or ignition).

A possible solution is a probe used as antenna for coupling into the cooking cavity. This concept allows also coupling to a rectangular waveguide, which makes the concept compatible to existing magnetron based appliances. When coupling directly into the cavity, a radome can be added to protect the electrical relevant parts, achieve leak tightness and fulfill further requirements on material properties as for example required by FDA rules.

Since the future will call for two or more amplifiers and antennas per appliance [1], mechanical construction gets more complex as well. Having a PCB-transition connected to a probe which is mechanically fixed to the cavity will impose significant mechanical stress between the used building blocks. This can be overcome by applying concepts known from board-to-board solutions (such as MMBX, MFBX and MBX). This way, mechanical stress is eliminated due to the given mechanical floating range, assembling is simplified due to the blind-mateability feature and electrical losses are reduced to very low level.

The above mentioned concepts are based on coaxial constructions. Moving towards alternative structures allows for additional cost saving at very high volumes. From this aspect having an antenna realized directly on the PCB (and thus on the same planar structure as the power amplifier is realized) is promising. Sealing to the cooking cavity can be realized by adding a dielectric low-loss material between the amplifier and the cavity.

One major disadvantage of this is however that the amplifier unit has to be placed very close to the cavity and the position is defined by the coupling location. This reduces design freedom significantly, and may lead to other limitations, for example caused by heat transfer. Adding a waveguide for gaining more design freedom makes sense from this perspective. A traditional rectangular waveguide with an antenna structure coupling into the antenna is what may came into designers mind when thinking in traditional solutions.

In order to gain features known from board-to-board solutions, such as mechanical freedom, blind-mateability, and having low-losses, as well as very good shielding properties, a launcher structure is beneficial. Also mechanical tolerances in the assembly process of the appliance are solved this way. From our perspective, realizing this with injection molded metalized parts, leads also to a very cost-efficient implementation. This concept allow also direct integration of additional functional elements like combiner or directional couplers, allowing mode and power control in dense packaging concepts

## CONCLUSION AND OUTLOOK

The concepts mentioned in this abstract show that most of the unsolved issues in the market can be addressed, including low-losses and good shielding properties, as well as cost and assembly requirements. Alternative connectivity concepts will contribute to achieve performance and cost targets required for a commercial solid state energy use in future. Features will further help to improve packaging, and mechanical aspects.

## REFERENCES


[1] RF Power Amplifier Roadmap: Residential Cooking, Version 2.0, March 2016, RF Energy Alliance.

[2] RF Coaxial Connectors, General Catalogue, Edition 2016/06, Huber+Suhner, Web: http://literature.hubersuhner.com/Technologies/Radiofrequency/RFConnectorsEN/

[3] RF Assembly Calculator, www: http://rfcablecalc.hubersuhner.com/, Huber+Suhner.

# Efficient High-Resolution Numerical Simulation of Microwave-Based Thermal Processes in Thin-Multilayered Domains by Using the PGD

**Hermine Tertrais[1], Ruben Ibanez[2] , Anais Barasinski and Francisco Chinesta[1]**

[1]GEM Institute, Ecole Centrale Nantes, Nantes, France
[2]ICI Institute, Ecole centrale de Nantes, Nantes, France

**Keywords**: Microwaves, Multilayered domains, Model Order Reduction, PGD.

## INTRODUCTION

Techniques based on the use of separated representations are at the heart of the so-called Proper Generalized Decomposition methods. Such separated representations were employed for solving multidimensional models suffering the so-called curse of dimensionality, transient models within a non-incremental integration schema and in the context of uncertainty propagation. Then, its use was extended for separating space coordinates making possible the solution of models defined in degenerated domains, e.g. plate, shells or multilayered domains; and finally for addressing parametric models where model parameters were considered as problem extra-coordinates. [1,2] The present work addresses the efficient solution of electromagnetic models related to microwave sources in multilayered materials. The high resolution required for accurately representing the electric field in the thickness direction makes impossible the use of well-experiences mesh-based discretization strategies like finite elements. The use of the in-plane-out-of-plane separated representation within the PGD framework allows reaching resolution levels never until now attained.

## ON THE USE OF SEPARATED REPRESENTATIONS

When using standard discretization techniques the solution is approximated in a certain given basis (polynomial in the case of finite elements) that despite of its generality are most of time poorly adapted to the solution to represent. Model reduction techniques proceed by extracting a suitable reduced basis (well adapted to represent the searched solution) on which the problem solution is projected. Thus, the reduced basis construction precedes its use, and one must be careful on the suitability of a particular reduced basis when employed for representing the solution of a particular problem different to the one from which the reduced basis was extracted. This issue disappears if the approximation basis is constructed at the same time that the problem is solved as discussed below.

When calculating the transient solution of a generic problem $u(x,t)$ we usually consider a given basis of space functions $N_i(x)$, $i = 1 \ldots N$ the so-called shape functions within the finite element framework, and approximate the problem solution as

$$u(x,t) \approx \sum_{i=1}^{N} a_i(t) N_i(x),$$

that implies a space-time separated representation where the time-dependent coefficients $a_i(t)$ are unknown at each time and the space functions $N_i(x)$ are given "a priori", e.g. polynomial basis.

POD and Reduced Bases methodologies substitute the general-purpose finite element basis $N_i(x)$ by a reduced basis, extracted from a training stage, $f_i(x)$, $i = 1,\mathrm{L}\ ,R = N$, instead of $N_i(x)$, for approximating the solution, according to

$$u(x,t) \approx \sum_{i=1}^{R} b_i(t) \phi_i(x).$$

Inspired from these results one could consider the general space-time, or even more general expressions when operating in the Fourier or Laplace spaces, from

$$\begin{cases} u(x,t) \approx \sum_{i=1}^{N} X_i(x) \cdot T_i(t) \\ u(x,\omega) \approx \sum_{i=1}^{N} X_i(x) \cdot \mathcal{W}_i(\omega) \\ u(x,s) \approx \sum_{i=1}^{N} X_i(x) \cdot \mathcal{S}_i(s) \end{cases}$$

respectively, where now all the involved approximations functions are computed on-the-flight when solving the problem, as widely described in [1,2].

By pushing forward this rationale we can express a 3D solution $u(x,y,z)$ as a finite sum decomposition involving lower dimensional functions

$$\begin{cases} u(x,y,z) \approx \sum_{i=1}^{N} X_i(x) \cdot Y_i(y) \cdot Z_i(z) \\ u(x,y,z) \approx \sum_{i=1}^{N} X_i(x,y) \cdot Z_i(z) \end{cases},$$

especially interesting when analyzing problems defined in plates or shell domains, or multilayered systems composed of numerous thin plies, as addressed in the present work.

In the case of models involving parameters the solution is expressed in a separated form involving the space coordinates, the time and the model parameters. That description is especially suitable for addressing real time simulation, optimization, inverse analysis, simulation-based control and uncertainty propagation as described in [1]. When model parameters are not so evident to define, machine-learning techniques can extract the uncorrelated parameters as discussed in [3].

## RESULTS

We consider a structural composite part 11 thin-layers plate geometry (thin with respect to the other characteristic dimension of the plate of one square meter) with orthotropic properties, one of the layers consisting of a perfect conductor. The plies arrangement is defined by $[0,90,0,\ldots,\text{conductor}]$, each ply 1 mm thickness. The material properties (permittivity and conductivity) for the plies oriented at 0-degrees (the ones oriented at 90 the properties are simply rotated) are two orders of magnitude higher than the ones along the orthogonal directions for the permittivity, i.e. $\epsilon_{yy} = \epsilon_{zz} = 4500 \,\&\, \epsilon_{xx} = 50$, and one order of magnitude for the electrical conductivity, i.e. $\sigma_{yy} = \sigma_{zz} = 100 \,\&\, \sigma_{xx} = 10$, with all the off-diagonal components of both tensors vanishing. The magnetic permeability is considered constant and unitary. A mesh consisting of $100 \times 100$ elements was considered in the plane and 111 elements were used for discretizing the domain thickness. Figure 1 depicts the electric field component $\mathbf{E}_x$ solution of the problem

$$\nabla \times \nabla \times \mathbf{E} = \gamma^2 \mathbf{E},$$

with $\gamma$ depending on the electromagnetic permeability, permittivity and conductivity, and in which the in-plane-out-of-plane separated representation previously introduced was employed and its high-resolution noticed.

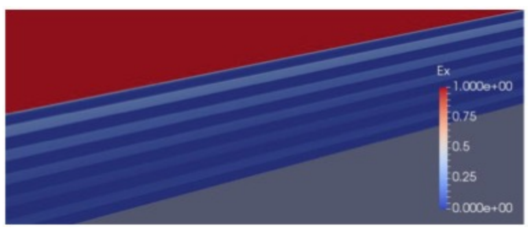


Figure 1. $\mathbf{E}_x$ – component of the electric field in a multilayered domain.

## CONCLUSIONS

The in-plane-out-of-plane separated representation allowed solving the electromagnetic field in multilayered plates of industrial relevance while capturing the rich behavior along the thickness direction. The associated computational complexity remains the one characteristic of 2D models, allowing fast and cheap solutions.

## REFERENCES

[1] F. Chinesta, A. Leygue, F. Bordeu, J.V. Aguado, E. Cueto, D. Gonzalez, I. Alfaro, A. Ammar, A. Huerta. Parametric PGD based computational vademecum for efficient design, optimization and control. Archives of Computational Methods in Eng., 20/1, 2013, pp. 31-59.

[2] F. Chinesta, R. Keunings, A. Leygue. Proper Generalized Decomposition for advanced numerical simulations. A primer. Springerbriefs, Springer, 2014.

[3] D. Gonzalez, J.V. Aguado, E. Cueto, E. Abisset-Chavanne, F. Chinesta. kPCA-based parametric solutions within the PGD framework. Archives of Computational Methods in Engineering. DOI 10.1007/s11831-016-9173-4.

# Comparison of Conventional, Induction and Microwave Based Thermo-catalytic Upgrading of Pyrolysis Vapors

**Pranjali D. Muley[1], Candice Ellison[1] and Dorin Boldor[1]**

[1]Louisiana State University Agricultural Center, Baton Rouge, LA, USA 70803

**Keywords**: Pyrolysis, microwave catalytic reactor, biofuels, thermo-catalytic upgrading

## INTRODUCTION

Pyrolysis of biomass has been proven to be an effective means for production of biofuels. Pyrolytic biofuel, however, has certain limitations. It is highly unstable, has high oxygen content and low energy density. Due to unstable nature of pyrolytic biofuel, it tends to polymerize during storage. Thermo-catalytic upgrading has proven to be an effective method for increasing biofuel stability. Catalytic upgrading reduces polymerization of biofuel during storage, decreases its oxygen content, and increases its energy density. Zeolites, more specifically H-ZSM-5 is most commonly used for biofuel upgrading. The common upgrading method includes heating the catalyst bed to an optimum temperature and the vapors react on the surface of the hot catalyst bed.

However, ineffective heating of the catalyst bed could result in undesired products and energy loss. Conventional heating techniques use external heat source for catalyst heating such as sand, which adds to the energy losses. Microwave heating uses catalyst as a dielectric source and generates heat within the catalyst without the use of external heat source. This increases the energy efficiency of the system. In this study, we compare three different catalyst heating methods; conventional, induction and microwave heating for optimum energy efficiency and biofuel upgrading.

## METHODOLOGY

Pyrolysis of pinewood sawdust was carried out at 600°C. The vapors from the reactor were passed over the hot catalyst bed. We studied the effect of three different catalyst bed temperatures (290°, 330° and 370°C) on upgrading of pyrolysis vapors using HZSM-5 catalyst as a model zeolite. The biomass to catalyst ratio was 2:1. The catalyst was reused for the second run of the same setting without regeneration and all experiments were performed in duplicates. Three reactors were studied;

1. Conventional reactor heating using a 13 mm x 1220 mm high temperature heavy insulated heating tape with 313 W output operating at 120 V surrounding the reaction tube.

2. Induction heating using a 5 kW RDO induction heater operating at frequency range of 135-400 kHz (RDO Induction LLC, Washington, NJ) to heat the catalyst bed.
3. Microwave heating using a 1.2 kW, 2450 MHz microwave system. A 2450 MHz microwave traveling wave applicator was modified to accommodate the catalytic bed. The reaction tube was made of quartz.

Biofuel, char and gas samples were collected and analyzed for yield and quality. Catalyst samples were analyzed for site activity.

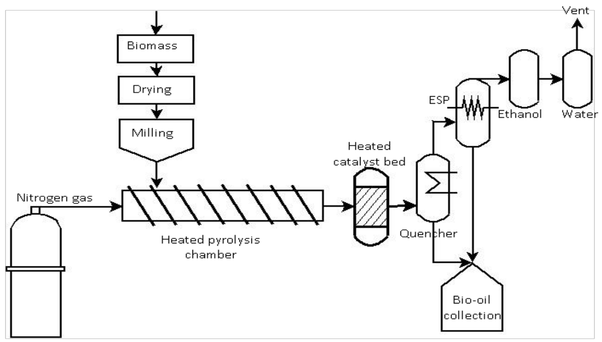


Figure 1. Flowchart for pyrolysis upgrading in a microwave heater

## RESULTS

A general observation for all three reactors was that as the temperature increases, liquid yield decreased. Catalyst activity decreased during the second run due to coke deposition from the first run. Microwave reactor performance exceeded the conventional and induction reactors in terms of aromatic yields, catalytic activity and energy requirements. At 370°C catalyst temperature, aromatics yield from the microwave reactor was 69.64% followed by the conventional and induction reactors (64.76% and 63.79% respectively).

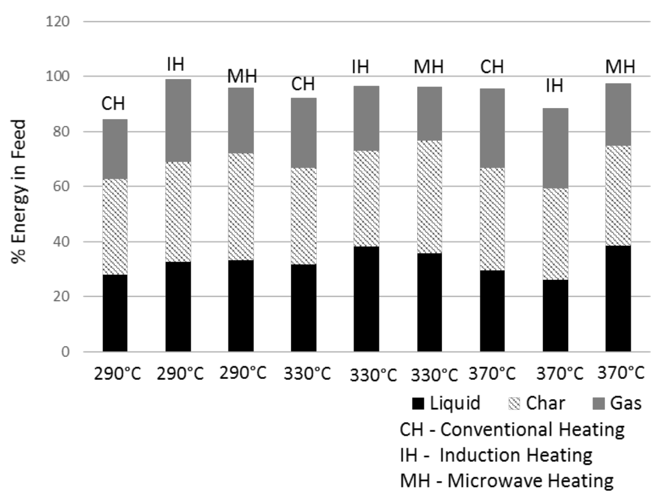


Figure 2. Percent energy in feed contribution by liquid, char and gas for three heating methods

| **Upgrading Temperature (°C)** | **Power Input for Catalyst Bed Heating (MJ)** | | | **Decrease in Energy Input in Microwave Heating (%)** | **Increase in Energy Efficiency Microwave Process (%)** |
|---|---|---|---|---|---|
| | Conventional Heating | Induction Heating | Microwave Heating | | |
| **290** | 0.6552 | 1.032 | 0.311 | 52.53 | 29.34 |
| **330** | 0.6552 | 1.290 | 0.3628 | 44.63 | 31.89 |
| **370** | 0.6552 | 1.806 | 0.4296 | 34.43 | 30.08 |

Table 1. Energy input and % efficiency of microwave heating

## DISCUSSION

Coke deposition on the catalyst was significantly higher for the conventionally heated catalyst at lower temperatures. This observation was reversed for the microwave heating method. Since, in a thermal cracking process, coke deposition increases as the temperature rises, coke deposition on the conventionally heated catalyst bed was a result of condensation of molecules on cooler catalyst regions rather than a byproduct of the reaction. Surface area analysis showed that used catalyst from the microwave reactor had highest available surface area, confirming lower coke deposition than the other methods. TPD analysis supported this observation as strong acid sites disappeared for the conventional heating method.

Microwave experiments yielded slightly higher heating values for biofuel compared to conventional heating. Energy required for microwave heating was lower and the energy efficiency increased by 35-50% compared to other heating methods. The induction heating method required the highest energy input. Overall, performance of the microwave reactor in terms of biofuel quality and energy efficiency exceeded both induction and conventional catalytic reactors.

## CONCLUSION

Microwave heating is an effective method for upgrading pyrolysis vapors and yields higher quality biofuel with lower energy input compared to conventional and induction heating methods. This technique should be further investigated to produce stable biofuel.

## REFERENCES

[1] Adjaye, J. D. and N. N. Bakhshi (1995). "Production of hydrocarbons by catalytic upgrading of a fast pyrolysis bio-oil. Part II: Comparative catalyst performance and reaction pathways." Fuel Process. Technol. **45**(3): 185-202.

[2] ASTM International (2014). Standard Test Method for Heat of Combustion of Liquid Hydrocarbon Fuels by Bomb Calorimeter. ASTM D240-14. West Conshohocken, PA, www.astm.org.

Al-Khattaf, S., C. D'Agostino, M. N. Akhtar, N. Al-Yassir, N. Y. Tan and L. F. Gladden (2014). "The effect of coke deposition on the activity and selectivity of the HZSM-5 zeolite during ethylbenzene alkylation reaction in the presence of ethanol." *Catal. Sci. & Technol.* **4**(4): 1017-1027

# Microwave Processing of a Laminated Part: Application to Glass Fiber Reinforced Polymer (GFRP)

**H. Tertrais[1,2], R. Ibanez[2], A. Barasinski[1] and F. Chinesta[2]**

[1]GEM, UMR CNRS - Centrale Nantes
Hermine.Tertrais@ec-nantes.fr Anais.Barasinski@ec-nantes.fr
[2]High Performance Computing Institute, Centrale Nantes
1 rue de la Noe, BP 92101, F-44321 Nantes cedex 3, France
Francisco.Chinesta@ec-nantes.fr

**Keywords**: Composites Processing, Microwave Heating, Thermoplastic Polymer, Proper Generalized Decomposition.

## INTRODUCTION

Composite parts tend to represent an increasing volume of production in transport industry due to their combination of high mechanical properties and low mass.

Inversely to traditional heating methods that depend on surface heat transfer and induce long cycle time, microwave (MW) technology relies on volumetric heating which enables better process temperature control [1] and less overall energy use, this can results in shorter processing cycles. The main drawback of this technology today is that the complex physics involved in the conversion of electromagnetic energy to thermal energy is not entirely understood and controlled.

The principal objective of this work is to model the interactions of the MW field with the composite material at micro and meso-scales, in order to simulate the way in which electromagnetic energy is converted to thermal energy within the material volume and the various interfaces. The main challenge concerns the high-resolution description of the electromagnetic and thermal fields in a composite laminate, that involve plies whose characteristic in-plane dimension is orders of magnitude higher than the ones related to the thickness (typical aspect ratio are of tens of thousands) (see Fig 1 left).

## PROCESS AND METHOD DESCRIPTION

The composite part to be heat is made of a GFRP, practically transparent to microwaves, it is placed on a bench, in a tool made of a material transparent to MW but coated in its interior surface by an absorbent layer. The whole is placed in an oven cavity with a hexagonal shape, as a Hephaïstos© one. The oven operates at a frequency of 2.45 GHz and has 12 magnetrons delivering a power up to 0.85 kW each.

A coupled thermal and electromagnetic model is proposed in order to simulate the composite materials heating. In that situation the use of in-plane-out-of-plane separated representations within the Proper Generalized Decomposition -PGD- framework, allows writing the electric field, using the Hadamard product, as:

$$\boldsymbol{E}(x,y,z) \approx \sum_{i=1}^{N} \boldsymbol{X}_i(x,y) \circ \boldsymbol{Z}_i(z)$$

This separated representation is especially interesting for addressing degenerated domains in which at least one of its characteristic dimensions is much smaller than the others, and the solution exhibits significant richness in the thickness direction implying the necessity of using a fine enough representation (mesh) to capture the transmission conditions at the ply interfaces. When using standard mesh-based discretization the use of a fine mesh in the thickness direction within a 3D discretization usually implies extremely fine meshes in the whole domain, involving a prohibitive number of degrees of freedom. The use of separated representations makes independent the in-plane and the thickness approximations, thus meshes in the plane and in the thickness can be refined independently. Such a separated representation seems an appealing and valuable route for solving 3D models, very rich in both, the in-plane and the out-of-plane directions, while ensuring a computational complexity of standard 2D models [2 -3].

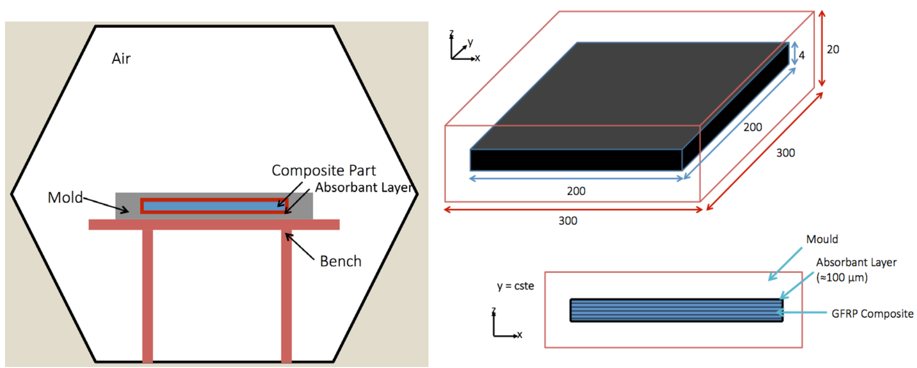


Figure 1. Schematic representation of the process (left) and zoom of the mould and composite part with its characteristic dimensions in mm (right).

## TEST CASE

We consider a domain made of GFRP (of dimension 4x200x200mm), surrounded by an absorbent box (100µm thick), and the whole surrounded by air (see Fig 1 right). The material properties of the GFRP and the absorbent layer are respectively the following (taken from the literature): $\varepsilon_r = 5$, $\sigma = 10^{-4}$, $a = 3.10^{-5}$; and $\varepsilon_r = 50$, $\sigma = 10^2$, $a = 10^{-4}$; with respectively the permittivity, conductivity (S/m), and thermal diffusivity (m²/s), the permeability $\mu$ is always $\mu_0$. The mesh is composed of 10000 elements in the in-plane (square elements whose length is 3mm) and 200 elements in the thickness direction (linear 1D elements whose length is 0.1mm). One must note that such degenerated mesh is not achievable with a classical approach (finite element for example). Figure 2 left depicts the electric field component $E_x$ evolution in the domain, and Figure 2 right, the associated temperature evolution after 1min.

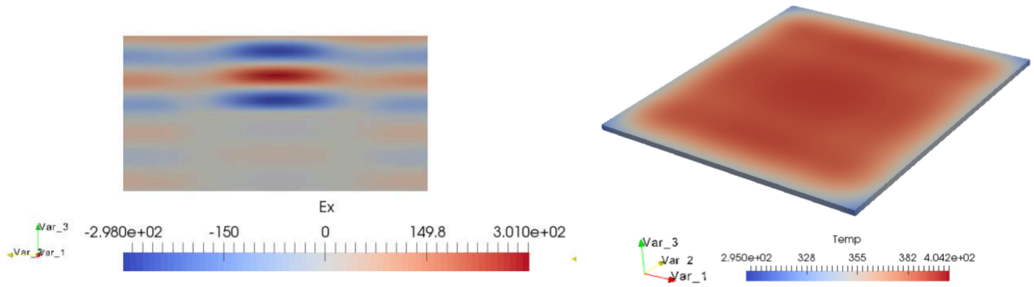


(a) (b)

Figure 2. Electric field component $E_x$ in the middle cross section of the whole domain (a) and Temperature evolution in the composite part (in Kelvin) after 1min (b)

## CONCLUSION

In the present work, a simulation tool is presented, allowing the calculation of the EM and thermal fields in the domain of interest, here being the composite part and mould domain placed into the oven cavity. These fine solutions will allow a better understanding of the thermal history experienced by the composite part during the heating stage in the microwave oven, and better defined the thickness of the absorbent layer, as well as the most appropriate material parameters by inverse engineering.

## REFERENCES

[1] G. Hug. (2005). "Behavior analysis of carbon-epoxy laminates under high-speed loading: manufacture of the same materials by means of microwave curing for comparison," Ph.D. thesis, Arts et Métiers ParisTech.

[2] B. Bognet, A. Leygue, F. Chinesta, A. Poitou and F. Bordeu (2012). Advanced simulation of models defined in plate geometries: 3D solutions with 2D computational complexity, Computer Methods in Applied Mechnanics and Engineering, 201, 1-12.

[3] F. Chinesta, R. Keunings, A. Leygue. Proper Generalized Decomposition for Advanced Numerical Simulations. A primer. Springerbriefs, Springer, 2014.

# High Efficiency Waveguide Applicators for Frequency Effect Studies

**Clayton DeCamillis and Iftikhar Ahmad**

**Lambda Technologies**
**860 Aviation Parkway, Suite 900, Morrisville, NC 27560**

**Keywords**: frequency effects, discrete frequency, swept frequency, high efficiency waveguide applicator, single mode applicator.

## INTRODUCTION

This paper is a tutorial on the design and operation of a high efficiency waveguide applicator for evaluating the frequency effect in various processes.

Microwave processing has been applied to a variety of processes in the past decades, which include but are not limited to chemical synthesis, plasma processes, microwave catalysis as well as processing of biomaterials and nanoparticles.

Almost all the work reported has been using fixed frequency microwave sources, primarily at 2.45GHz. It is well known that microwave absorption is influenced by frequency. For example, in the area of plasma processing Szebo [1] reports a relation between the collision frequency and transferred energy to plasma elementary species at common microwave frequencies, 0.915 GHz, 2.45 GHz, and the less common industrial frequency 5.85 GHz. With increasing frequency the transferred energy decreases. Consequently, for nanoparticle synthesis with microwave plasma, a lower microwave frequency leads to higher reaction temperatures, while lower synthesis temperatures can be realized with higher frequencies. This notion calls for a microwave plasma system capable of varying the frequency.

Furthermore many of these processes can involve metallic or metal particle bearing catalysts that can arc or suffer localized hot spots under fixed frequency. Swept frequency processing resolves these issues and is a natural fit.

Frequency effects are being explored utilizing a new design of the tried and true waveguide applicator combined with high power broadband frequency sources.

 

## HIGH EFFICIENCY WAVEGUIDE APPLICATOR

The core design is based on a traditional traveling wave mode applicator coupled with features that enable standing wave operation at a wide range of frequencies. Broadband solid state and traveling wave tube sources power the system. Process tubes are used to stage catalysts and/or carry reactant fluids through the applicator. The process tube can also provide vacuum capability and with a gas feed can be used for plasma generation.

Details will be provided on a unique approach to designing the applicator, the selection of tuning components, the control of high power broadband microwave sources and techniques for process control feedback.

## RESULTS

Experimental results with variable frequency high power sources show excellent coupling over a broad range of fixed frequencies. Operational systems span the range of 2.4 to 8.0GHz with multiple applicators. System design allows tuning to standing wave operation at virtually any discrete frequency. The system can also support operation in traveling wave mode, and importantly the introduction of a variable bandwidth of frequencies. This allows identifying a best center frequency and then sweeping around that center frequency for a robust and sustainable process for small scale reactions.

## CONCLUSION

For academic investigations this apparatus will be advantageous to explore optimum frequencies for a particular reaction. For industrial production where there may be fluctuations in the pressure and gas flow, broader bandwidth operation should provide increased stability without the loss of coupling.

## REFERENCES

[1] Szebo D. et.al., "Microwave Plasma Synthesis of Materials-From Physics and Chemistry to Nanoparticles: A Materials Scientist's Viewpoint", Inorganics, 2, pp.468-507, 2014.

# Switched Parasitic Antennas for Microwave Mode Stirring

**Gregory J. Durnan**[1]

[1]NXP Semiconductors, Chandler, Arizona, USA

**Keywords**: oven, cavity, mode, stirring, parasitic, antennas.

## INTRODUCTION

Presented is a study of the use of parasitic antennas (scatterers) within the cooking cavities of commercial and consumer microwave ovens. In particular we look at the use of switching these scatterers in and out of system via the use of pin diodes for the purpose of mode stirring with a view to improving the evenness of the microwave cooking experience. Experimentally we look at the use of patch antenna's as the basic switched element but the work can be extrapolated to other elemental line and aperture antenna types, such as dipoles, monopoles and hairpins [1,2].

The use of parasites to redistribute the energy within the cavity has been the subject of a number of historical patent applications [3,4] in order to focus or redistribute the energy within the cavity. In addition, at the present time, it is a commonly used feature in some food packaging such as in frozen pies (meat/pot & fruit) to include a resonant parasitic disk to raise the electric field component in a particular location such that browning and crisping may occur (accelerated cooking in the parasite location). Other uses include concentrating the field to ensure improved pop-corn cooking such as in Figure 1a. In this paper we take an extra step of switching these parasites in and out of resonance so that we may control them via the cooking algorithm of a microwave oven, particularly one with solid state control.

In addition to their use as E field concentrators and scatterers, parasites may also hold some promise in solid state ovens as a means to add extra source locations within the cavity without having to increase the number of directly driven feed locations (for mode purposes) which otherwise may be cost prohibitive.

## METHOD AND SIMULATION

The problem was initially examined using CST Microwave Studio as the simulation environment and an examination was made of the total E field as a mid cut through both load and antennas, as shown in Figure 1b. Once the basic structure was configured a study of the placement of a number of parasites, from none to 3 was performed and compared to each other and to experimental results using color changing desiccant within the cavity.

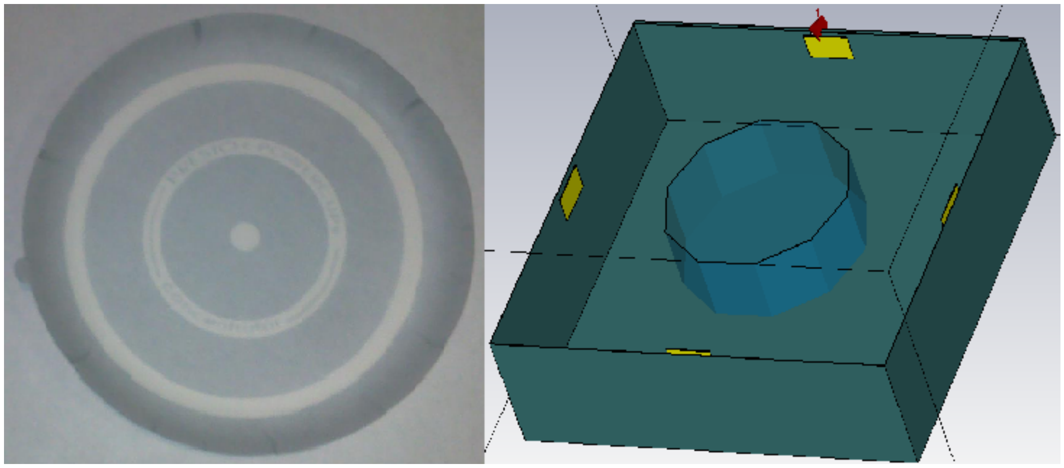

(a) (b)

Figure1. (a) A currently available parasitic element (Presto Power Pop™ ) (b) The CST simulation structure - showing one driven element and three parasites.

## RESULTS

The addition of a number of parasites was simulated to show that, in comparison to a single driven element, additional modes appeared to be excited throughout the cavity, and those modes appeared to be excited around the circumference of the load in a more uniform fashion. The parasitic patches are clearly seen with raised E fields (fringing fields) and so there is considerable excitation shown in Figure 2b versus 2a.

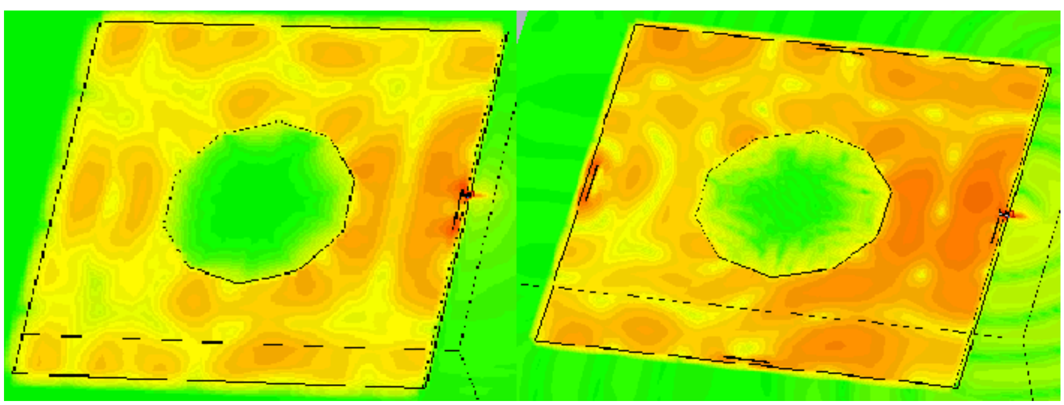

Figure2. (a) Simulated cavity behavior showing one driven patch antenna (b) Simulated cavity behavior showing one driven patch antenna and an additional 3 parasitic patches.

## DISCUSSION

Placement and number of parasites suggest that some parasites are excited to a greater degree than others, supporting the use of switched parasites to optimize for a given load shape. A method of sensing may be of interest in determining the level of excitation in relation to a given load. Studies in this area may help develop improved cooking algorithms, particularly for consistent even cooking.

Several techniques can be used to switch these parasites but the author has concentrated on methods that detune the patch antenna, essentially shorting part of the antenna to the cavity via the use of pin diodes. Such an arrangement can be seen in Figure 3.

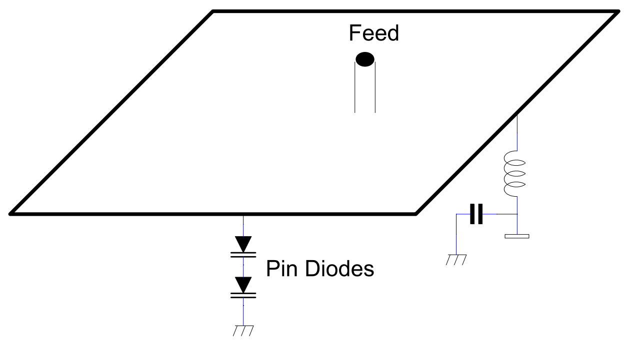


Figure 3. Patch Antenna with series pin diodes to switch the radiating fringing fields to ground

Several options for switching mechanisms have been tried but it was found that placing the pin diodes in series reduced the capacitive detuning effect under normal operating conditions and allowed for higher breakdown voltage levels. Placing the DC supply along the non-radiating edge was considered preferable to avoid any potential arcing. These were in practice added in a series configuration as well to avoid self resonance and also to provide a larger voltage gap. Figure 2. shows changes in field patterns due to placement of the switched parasitics but these changes of course are highly dependent on the loading conditions. Some work has been performed with parasites switched in close proximity to the food (at each corner) and with some clarity we can see the E-Field and heating levels rise at those locations around the food surface.

## CONCLUSION

The use of parasitics was revisited in this paper, and in particular the active switching of these parasites in order to promote mode stirring, additional mode excitation and the sensing and use of this parasitic behavior with a view to developing improved cooking algorithms suitable for maintaining even cooking performance.

## REFERENCES


[1] D.V. Thiel and S. Smith,*Switched Parasitic Antennas for Cellular Communications*, Artech House, MA, 2002.

[2] G.J. Durnan, D.V.Thiel, S.G. O'Keefe, *Switched Parasitic Feeds for Parabolic Antenna Angle Diversity,* Microwave and Optical Technology Letters, John Wiley, November 20. 1999

[3] E.J.Kajewski, Litton Industries, *Microwave Heating Apparatus*, US Patent 3271552, Sept. 6, 1966.

[4] H.C. Anderson, Litter Systems, *Mode-Shifting System for Microwave Ovens*, US Patent 3740514, June 19, 1973.

# The Response of Silver Beet to Microwave Generated Biochar

**Graham Brodie, Bhawana Bhatta Kaudal, and Cristina Aponte**

[1] Dookie Campus, The University of Melbourne, Australia

**Keywords**: Waste, Microwave, Biochar, Plant growth.

## INTRODUCTION

In the five-year period 2008-2013, Australian biosolids production, derived from sewage sludge, increased from approximately 300,000 dry tonnes [1] to 330,000 dry tonnes [2]. During this time, the proportion of biosolids disposed of with beneficial use increased from 59% to 69%. The majority of this increase was due to the diversion of biosolids from landfill to land application as a low grade nutrient source for crop and pasture production, particularly in the states of Queensland and New South Wales [2]. Of the 102,000 tonnes of dry biosolids that were not beneficially used in 2013, 62% was produced by the state of Victoria, with the majority placed into stockpiles [2]. The current size of the Victorian stockpiles, which have been in use for many years, is estimated at 3.2 million dry tonnes.

Pyrolysis of organic materials yields: syngas; bio-oil; and biochar [3-5]. Syngas is a combustible fuel; bio-oil has a number of potential applications, depending on the chemical composition of the oil; and biochar has recently been used as a soil ameliorant in agricultural systems.

Biochar has commonly been generated using conventional convective heating in furnaces; however, the use of this method to pyrolise biosolids is deterred by the high moisture content of this material and often requires the inclusion of a substantial fraction of wood chips in the biosolids to achieve successful pyrolysis.

Microwave energy offers a better alternative to conventional convective heating for the pyrolysis of biosolids because of its processing speed and ability to cope with the high moisture content of biosolids. If previously generated biochar is added to the raw material as a susceptor, there is no need to acquire wood chips for the pyrolysis process. Thus microwave heating can generate biochar from biosolids more efficiently; however, previous work has shown that biochar, derived from the conventional pyrolysis of biosolids, had no beneficial influence over plant growth and the potential of this microwave generated biochar, as a growth medium for plants, has not been explored. This study investigated the effect of microwave generated biochar on growth media leachates and plant growth in a glass house experiment.

## METHODOLOY

Biosolids, acquired from the Euroa (36° 45’ S, 145° 34’ E) municipal waste water treatment plant, were treated in a 6 kW, 1 $m^3$, multi-magnetron, multi-mode, microwave chamber at Dookie campus of the University of Melbourne. The mass of these samples were approximately 2340 g. The samples were broken up using a food blender, thoroughly mixed with about 10 % by mass of biochar that was produced from the same biosolids in earlier experiments, and placed into a 4-litre fused quartz crucible with a close fitting lid which limited the amount of oxygen available during the treatment.

Samples were placed into the multi-mode chamber with the input microwave power set to maximum (6 kW).

Pyolysis was assumed to have commenced when smoke and volatiles were observed in the air-steam exhausting from the chamber. Treatment was allowed to continue for a further 10 minutes to ensure the pyrolysis reaction was completed and all the biosolids material was charred. A thermal camera was used to record the temperature of the system and the samples after treatment.

A replicated pot experiment was used to evaluate the value of microwave created biochar. Biochar was tested as a growing media substrate in four treatments: T1 – Control, which consisted of 20 % sphagnum peat and 80 % pine bark (with fertiliser added); T2 – 20 % Biochar and 80 % pine bark (with fertiliser); T3 – 60 % Biochar and 40 % pine bark (with fertiliser added); and T4 – 60 % Biochar and 40 % pine bark (with no fertiliser added). Silver beet (*Beta vulgaris* L.) plants, one per pot, were used as a test species. A basal dose of a micronutrient solution (Mg, Mn, Bo, Fe, Cu, Zn at rates of 50, 20, 18, 18, 18, 18 kg $ha^{-1}$ equivalents) as $Cl^-$ and $SO_4^{2-}$ salts was applied to all treatments except treatment 4 on the first day of the experiment. Weekly doses of N (as $NH_4NO_3$), P (as $KH_2PO_4$) and K (as $KH_2PO_4$ and KCl) (total 89, 33, 39 kg $ha^{-1}$ equivalents) were applied to each chamber according to department of agriculture, Western Australia's recommendations for vegetable crops [6]. Final plant biomass and leachate of nitrogen and phosphorus from the specially constructed pots were measured.

## RESULTS

Immediately after the microwave treatment process, the outer temperature of the quartz crucible was consistently between 300 °C and 350 °C; however, the samples were consistently between 600 °C and 650 °C. The microwave chamber reached an external temperature of between 35 °C and 40 °C during the experiment. It should be noted that no insulation was used or required in the chamber during these experiments; however, welding gloves were used to handle the hot samples. These temperatures are consistent with the volumetric heating behaviour of microwave processing, where the sample is heated, but not the environment [7].

Nitrate and $NH_4$ leachate losses were the lowest in T2 (20% biochar plus fertiliser; Figure 1). Phosphate losses were observed in the control treatment (T1) but were negligible in all biochar treatments, regardless of the addition of fertiliser. This result suggests that biochar helped in retaining nutrients and potentially makes them available for plant uptake.

Plant dry weight differed significantly between treatments with the highest root and shoot biomass observed for T3 (60% biochar plus fertiliser; Figure 1). In contrast, plants in T4 (60% biochar, no fertiliser) were the smallest both in root and shoot biomass, suggesting that biochar itself has little nutrient value. Plants grown in T2, which was the treatment with the lowest nutrient leachates, were also larger than those in the control treatment (T1), but differences only occurred in their aboveground biomass, with root biomass being similar to the control.

Heavy metals such as Cd, Cr, Ni and Pb, which could potentially deter biochar use as soil amendment because of their toxicity, were below the detection limit of 0.1 mg $g^{-1}$ for all plant and media leachate samples. Other heavy metals such as Cu, Zn, Mn were all below EPA classification, which safely allows microwave created biochar to be used as a growing media.

## CONCLUSION

Microwave assisted pyrolysis of sewage biosolids produces biochar, which can be used as a growth media for plants. This media helps to retain nutrients and significantly enhances plant growth.

## REFERENCES


[1] R. J. LeBlanc, P. Matthews and R. P. Richard, *Global atlas of excreta, wastewater sludge, and biosolids management: moving forward the sustainable and welcome uses of a global resource* Un-habitat, 2009.

[2] Anonomous, *Fact sheet - biosolids profile ed*, Canberra, 2013.

[3] J. Aimin, C. Yan, L. Hongya and Q. Zuguo, A Review on Pyrolysis Technology and Characters of Products from Sewage Sludge, *Applied Mechanics and Materials,* vol. 295-298, pp. 1419-1424, 2013.

[4] S. Luo, Y. Zhou and C. Yi, Syngas production by catalytic steam gasification of municipal solid waste in fixed-bed reactor, *Energy,* vol. 44, no 1, pp. 391-395, 2012.

[5] V. Kirubakaran, V. Sivaramakrishnan, R. Nalini, T. Sekar, M. Premalatha and P. Subramanian, A review on gasification of biomass, *Renewable and Sustainable Energy Reviews,* vol. 13, no 1, pp. 179-186, 2009.

[6] J. Burt, *Growing silverbeet in Western Australia*, Western Australia, 2005.

[7] G. Brodie, The influence of load geometry on temperature distribution during microwave heating, *Transactions of the American Society of Agricultural and Biological Engineers,* vol. 51, no 4, pp. 1401-1413, 2008.


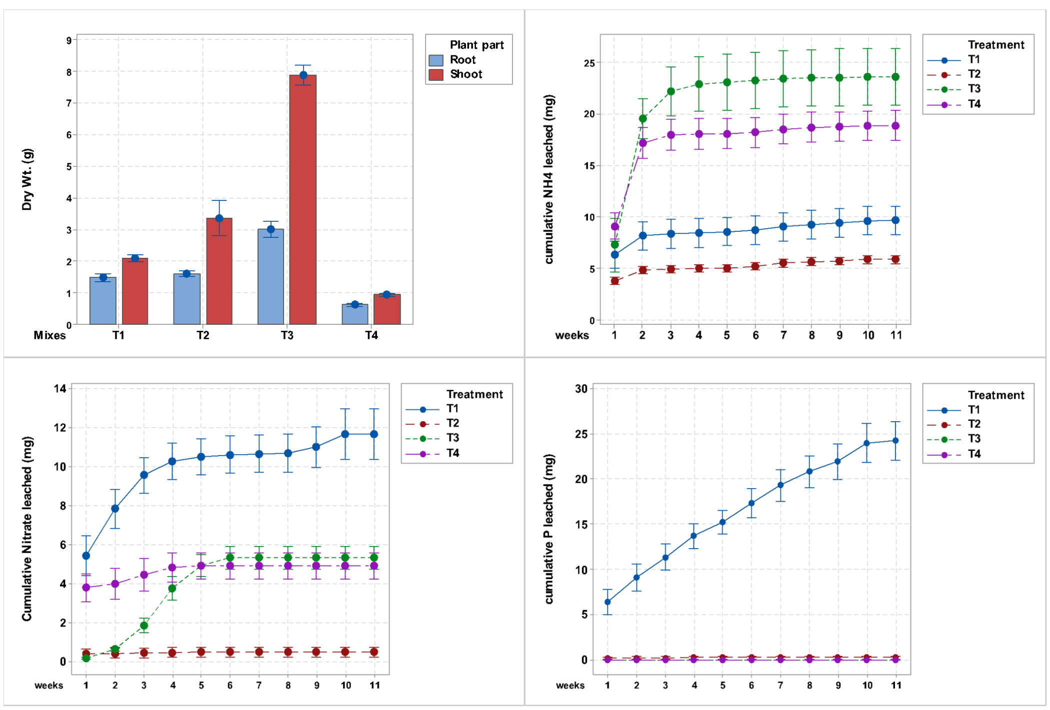


**Figure 1.** Results from plant growth experiment – (top left) biomass – (top right) cumulative NH4 leachate – (bottom left) cumulative nitrate leachate – (bottom right) cumulative phosphate leachate

# Residual Effect of Microwave Soil Treatment on Growth and Development of Wheat

**Muhammad Jamal Khan, Graham Brodie, Dorin Gupta and Jim He**

The University of Melbourne, Dookie, Australia

**Keywords:** Microwave, Soil, Persistence effect, Wheat yield

## INTRODUCTION

Microwave soil treatment for weed suppression and crop growth has been evaluated during the last decade in Australia. Numerous studies have reported a profound effect of pre-sowing microwave soil irradiation on weed seed emergence [1] and subsequent crop growth and yield [2]. However, the residual influence of a once-off 2.45 GHz microwave soil treatment on crop growth and yield is still unclear. A glasshouse study was conducted to examine the residual effect of microwave irradiation of the soil on subsequent wheat growth and yield in a second season.

## METHODOLOGY

A two factorial, completely randomized block design glasshouse experiment was conducted with ten replicates of each treatment combination at the Dookie Campus of the University of Melbourne, Australia. The soil, classified as clay loam, was treated ($T_0$= Control and $T_1$= 120 s) in a bench-scale microwave oven with cavity dimensions of 370 × 380 × 210mm during the 24th – 27th of August, 2015, and was subjected to four levels of isotopic nitrogen ($N_1$ = 0 mg $^{15}N\ L^{-1}$, $N_2$ = 50 mg $^{15}N\ L^{-1}$, $N_3$ = 100 mg $^{15}N\ L^{-1}$ and $N_4$ = 150 mg $^{15}N\ L^{-1}$) application to estimate nitrogen use efficiency in wheat crops. After the completion of this first experiment, the soil remained undisturbed for 4 months in the same pots and same variety of wheat (Gregory) was sown on 6th of June, 2016. Monoammonia phosphate (150 kg $ha^{-1}$) was applied to each pot as a starter dose for wheat production. Four plants were harvested from each pot at the maximum tillering stage for fresh weight and dry weight measurements. The final dry biomass yield and grain yield was measured at crop maturity.

## RESULTS

Microwave irradiation of soil significantly increased the dry biomass yield (Figure 1) and grain yield (Figure 2) of a subsequent wheat crop harvested 300 days after irradiation under all levels of nitrogen application in a glasshouse experiment. Wheat growth in control and treated pots at the tillering stage is compared in Figure 3.

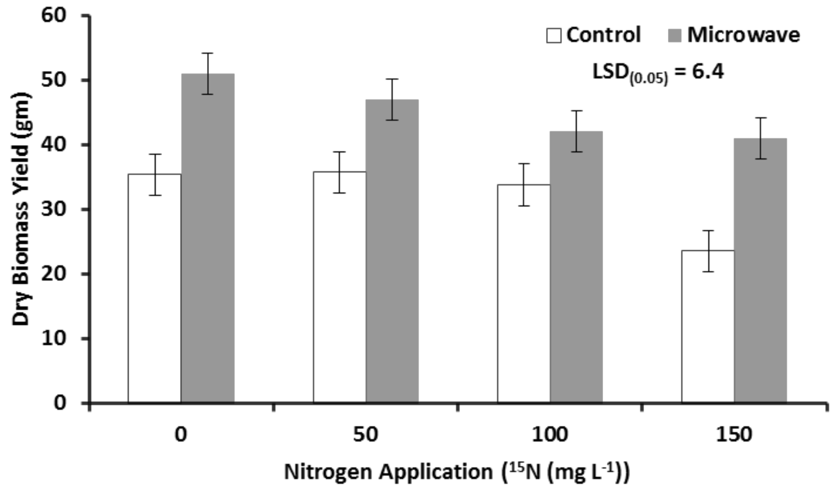


Figure 1. Residual effect of microwave (2.45 GHz & 120 s) soil treatment on the dry biomass of a subsequent wheat crop under various level of isotopic nitrogen application.

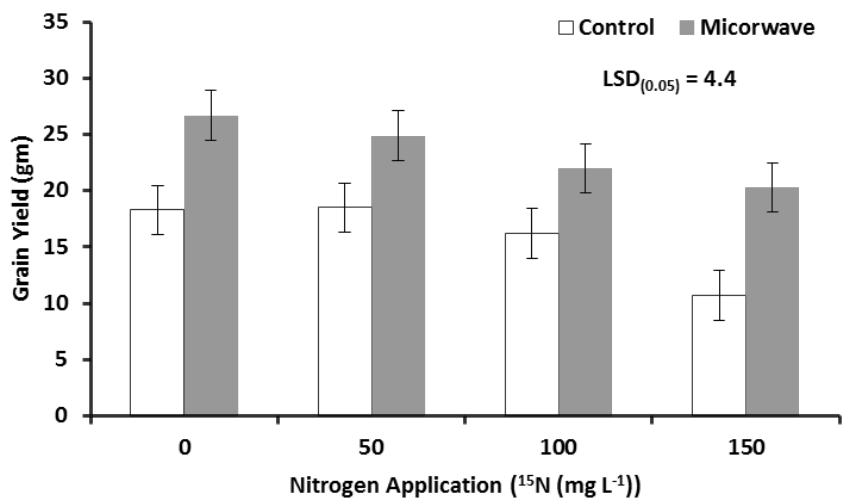


Figure 2. Residual effect of microwave (2.45 GHz) soil treatment on grain yield of a subsequent wheat crop under various levels of isotopic nitrogen application.

Figure 3. Persistent effect of microwave soil treatment (2.45 GHz, and 120 s) on the growth of a subsequent wheat crop. The microwave treated pot on the left with no nitrogen application had dark green expanded leaf area and 2 – 3 tillers plant$^{-1}$, while the untreated control pot on the right with a full a nitrogen dose (150 $^{15}$N (mg L$^{-1}$ )) had only main shoots and no tillers. N increased the crop growth and development in first season of application, but the nitrogen fertilizers applied in this study had has little residual influence in the following season.

## DISCUSSIONS

The long lasting effect of microwave soil treatment on crop growth may be due to microwave induced degradation of soil organic matter. The higher amount of substrate in the soil may enhance microbial activity, which ultimately increases the soil fertility. This persistent effect of microwave soil treatment could reduce the amount of fertilizer needed in the cropping system not only in first crop but also in a subsequent crop in the next season.

## CONCLUSIONS

Based on the result of this investigation, we conclude that microwave soil treatment has a supplementary benefit in the improvement of crop yield in both the first and a second crop, in addition to weed management. However, although a reason for this benefit is suggested, it must be verified and further investigated.

## REFERENCES

[1] I. Sartorto, G. Zanin, C.Baldoin and C. De-Zanche, Observations on the potential of microwaves for weed control.*Weed Res.* vol. 46(1), pp. 1-9, 2006.

[2] G. Brodie, N. Bootes and G. Reid, Invited Paper. Plant growth and yield of wheat and canola in microwave treated soil, In *IMPI's 49th Microwave Power Symposium*, San Diego, California, USA, 2015, pp. 40-41.

# Benefitting of Plants Using Microwave Genetic Activation Method and its Applications

**Satoshi Horikoshi, Yasuhiko Hasegawa and Nobuhiro Suzuki**

Department of Materials and Life Sciences, Faculty of Science and Technology, / Microwave Science Research Center MSRC, Sophia University, 7-1 Kioicho, Chiyodaku, Tokyo 102-8554, Japan, e-mail: horikosi@sophia.ac.jp

**Keywords**: Microwave genetic activation method, Growth acceleration, Arabidopsis thaliana, Molecular biology

## INTRODUCTION

We found that when plants are irradiated with microwaves for several minutes during the early growth stage their growth rate is enhanced. This paper considers why growth was promoted by microwave irradiation from the angle of the molecular biology. Our results suggest that effect of the microwave on plant growth is non-thermal. Elucidation of a key factor that underlies microwave-dependent growth stimulation of plant is essential for the application of this techniques to other plant species (potato, corn, switch glass, etc), because regulatory mechanisms for a broad range of important biological processes are highly conserved among the various plant species. In additional advantage of this method may be high survival rate in a disadvantageous environment (combination of drought and the high temperature). To scale up this method, several applications were performed using a semiconductor microwave generator.

## METHODOLOSY

A model plant, *Arabidopsis thaliana* was grown in potting compost (Jiffy 7, peat pellet) under controlled conditions (21 ºC and 16-hrs light) in a growth chamber for 14 days until the beginning of the emergence of the 1st true leaves. Microwave irradiation that did not alter the leaf temperature (23W) or heat treatment (40 ºC) using a conventional heater was applied for 1 hour on seedlings. Then, the plants were grown under controlled conditions in the chamber following those treatments. The atmospheric temperature and light intensity were uniform for all samples. The extent of growth promotion was evaluated by scoring the size of leaves, inflorescence stem length, timing of flowering and seed germination rate. And, total amount RNA and protein extracted from plant samples and the expression of genes or proteins involved in the regulation of growth and stress responses were analyzed by the Reverse Transcription Polymerase Chain Reaction (RT-PCR) and Real-Time Polymerase Chain Reaction (Real Time PCR), or Western-blotting, respectively.

**RESULTS＆DISCUSSION**

Because the growth of an inflorescence stem was promoted by microwave irradiation, expression of genes and proteins involved in the regulation of flowering were analyzed. It was confirmed that expression of the FT (FLOWERING LOCUS T) protein that controls the timing of flowering is enhanced by microwave irradiation at the 22nd day after seeding (Figure 1). On the other hand, expression of genes encoding MYB30 (MYB domain protein 30) and CO (CONSTANS) protein that regulate FT gene expression did not increase. A CO gene is associated with the photoperiod, and MYB30 gene is not linked to the photoperiod. This suggests that the microwave irradiation did not influence the circadian clock. Arabidopsis irradiated on the 14th days after seeding had enhanced tolerance to a combination of drought and heat stress at the transition from the vegetative to the reproductive stage at 28 days after seeding. The transition to the reproductive stage is important for a plant to produce a seed, and a plant's profitability is enhanced by its ability to acclimate to stressed conditions at this stage [1]. Under the combined stress employed in this study, it was confirmed that microwave irradiation increased the survival rate by 30% (Figure 2).

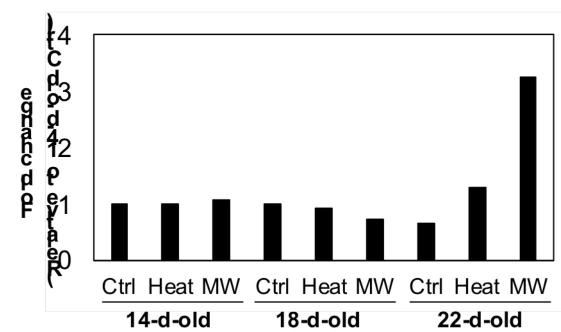


**Figure 1** Expression of FT protein analyzed by Western blotting. Values were normalized by expression of RubisCO as an internal control. "Ctrl", "Heat" and "MW" represent non-irradiated control, conventional heat and microwave, respectively.

**CONCLUSION**

Plant growth can be promoted by a microwave irradiation, and it might be different from the effects caused by heat stress. This technology is also effective to other plant.

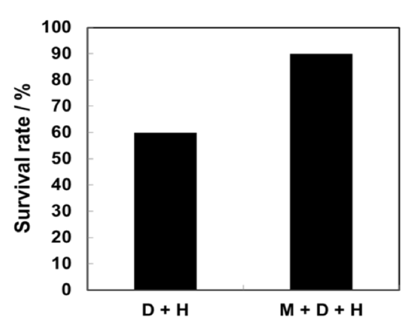


**Figure 2** Survival rate of the plants under the drought and heat stress without microwave irradiation (D+H) and drought and heat stress with microwave irradiation (M+D +H).

**REFERENCES**

[1] Kemal Kazan, Rebecca Lyons, *Journal of Experimental Botany*, **67** (2016), 47–60.

# Novel Microwave System for Uniform Processing of Food

**P. Swiergon[1], M. Gamage[1], P. Sanguansri[1], K. Knoerzer[1], N. Tran[2]**
[1] CSIRO Agriculture and Food, 671 Sneydes Road, Werribee, VIC, Australia
[2]Microwave Power Components, 11 Tannery Road, Charlemont, VIC 3217, Australia

**Keywords**: Industrial microwave, antenna loop, food processing, heating protocols.

## INTRODUCTION

Food products generally have complex geometries and non-uniform dielectric property. The final product quality and heating efficiency are highly dependent on the distribution of the electromagnetic field within the microwave system. An ideal microwave oven should heat all products evenly, but non-uniform distribution of the electromagnetic field and the formation of standing waves, among other factors, can result in cold and hot spots within the food product The uniformity of the field distribution may be estimated theoretically from the number of modes that may be excited within a narrow frequency range close to the magnetron frequency, or studied experimentally [1].

Currently patented solutions to overcome the uneven heating issue in commercial microwave systems include rotating turntable, mode stirrer, polyhedron chamber or strip line antenna. The team at CSIRO has developed a new solution using a regulated power control, quasi-elliptic chamber and a helical antenna to address the uneven heating of food products [2].

## METHODOLOY

Each module of the prototype microwave chamber (Figure 1a) contains 2 microwave generators on each side attached to an antenna loop. A simultaneous electromagnetic and thermal solver, implemented in Microwave Studio™ (Computer Simulation Technology, USA), was used (Figure 1b) to assess the performance of the single chamber module [3].

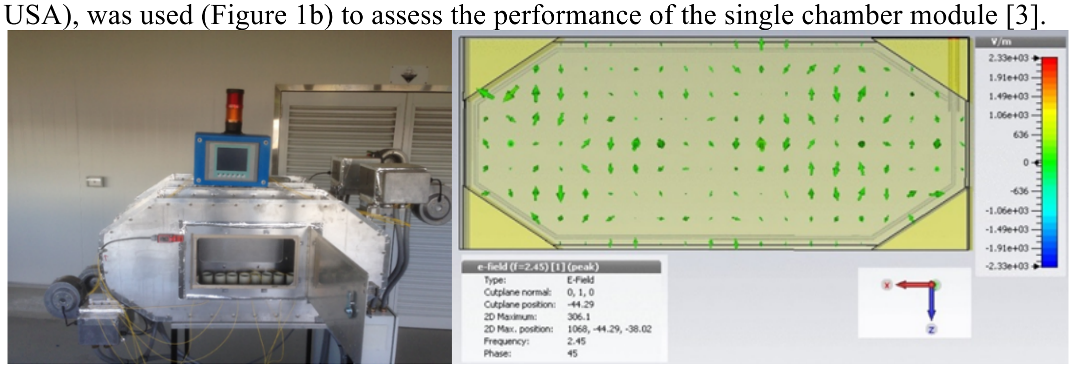


Figure 1. CSIRO Antenna Microwave Chamber: Picture of twin cell prototype unit (a) and CST simulation result (b).

Zucchini fruits were used to test this prototype during commissioning, to compare with our previous disinfestation trials [4]. Heating protocols were developed to heat the fruit to different target temperatures at the slowest heating point. The quality of treated and untreated zucchini (Figure 2) samples were evaluated on day 1, 6, 9, 12.and 15.

## RESULTS


Figure 2. Photographs of untreated (left) and microwave treated (centre) zucchini from quality trials on day 12, and temperature profile (right).

## DISCUSSION

The external quality of the MW treated zucchini was comparatively better than in previous insect disinfestations experiments [4] conducted with a pentagonal microwave unit.

## CONCLUSION

The Multiphysics simulation of a twin cell antenna microwave chamber shows an improved distribution of the electromagnetic field in the cavity and consequently a more uniform temperature increase. However, for high uniformity application such as disinfestation further optimizations of microwave sources that take full advantage of the microwave antenna design will be required.

## REFERENCES

[1] M. Vollmer, Physics of the microwave oven, *J. Physics Education*, vol. 1, pp. 74–81, 2004.
[2] P. Swiergon, P. Sanguansri, M. Gamage, K. Knoerzer, X. Xinqing, N. Tran, CSIRO. Microwave heating apparatus, Prov. Patent, 2015903603 AU/PROV, 2015.
[3] CST STUDIO SUITE™ 2008, Application and Feature Tutorial, EM Thermal Co-Simulation.
[4] T.V. Gamage, P. Sanguansri, P. Swiergon, M. Eelkema, P. Wyatt, P. Leach, D.L.J. Alexander, K. Knoerzer, Continuous combined microwave and hot air treatment of apples for fruit fly (Bactrocera tryoni and B. jarvisi) disinfestation, *Innovative Food Science and Emerging Technologies*, vol. 29, pp. 261–270, 2015.

# Food Processing with Microwave for Industrial Applications

**Klaus M. Baumgaertner[1], John F. Gerling[2] and Markus Dingeldein[1]**

[1]MUEGGE GmbH, Reichelsheim, Germany
[2]MUEGGE-GERLING, Modesto, USA

**Keywords**: Food Pasteurization, Food Sterilization, Microwave Heating, Solid State.

## INTRODUCTION

In recent years, the amount of ready-to-eat food products sold worldwide has been steadily increasing. This trend is driven by the growing need for greater convenience due to the increasing complexity of schedules and time demands on families and individuals. In parallel to this trend, a growing number of consumers are demanding higher-quality foods. High quality in food is associated with improved freshness and preservation of nutrients, e.g. vitamins in particular.

Combining ready-to-eat food products and high quality nutrition still is and will increasingly be a challenge for the food industry. One of the major challenges is to find the best balance between food preservation and food quality. Pasteurization is increasingly being selected as opposed to sterilization due to consumer trends and requirements. This transition will accelerate even more rapidly as new microwave pasteurization processes provide additional improvements towards food safety as well. After presenting different examples of industrial food sterilization and pasteurization by application of microwaves, this paper will focus on the particular specifications of food pasteurization to be met by microwave technology.

## METHODS AND APPLICATIONS

A wide variety of microwave applications can be found in the food industry, e.g. dehydration, baking, tempering, and heating. It is not only simple cooking by injection of microwave energy, microwave technology is even used for “modification” of food products, which can be found in popping up of cereals for example. Regarding preservation of food products, microwaves can be applied in different ways, too. Shelf life of food can be extended by microwave assisted brine injection, applied on meat and fish in particular, in a dehydration process or by “ordinary” heat sterilization or pasteurization by means of microwaves. Short process times and relatively homogeneous tempering and heating of the bulk and not only of the surface are major advantages of microwave technology in food sterilization and pasteurization.

Nowadays and more increasingly in the future, preservation of nutrients will be as important as extension of shelf life for consumers worldwide. This will drive the transition from sterilization processes towards pasteurization. In conjunction with this change, there will be new challenges for microwave technology. Reducing the temperature of the process to a minimum of 70 °C and a maximum of 90 °C, pasteurization processes require a more precise dosing of the microwave energy compared to sterilization processes. Focusing on ready-to-eat products consisting of various kinds of food materials, the dielectric constants $\varepsilon'$ and the dielectric loss factors $\varepsilon''$ of the different food components determine their ability to store electric energy and the conversion of microwave energy into thermal energy, respectively [1]. In extreme cases, the temperature of one food component can already be close to decomposition of its nutrients while the temperature of another food component is still below the threshold necessary for pasteurization after microwave heating. For avoidance, anisotropic launching of the microwave and controlled variation of the microwave frequency within the limits assigned by the local authorities can be envisaged. This will require new microwave antenna concepts and application of solid state technology for microwave generation. Simulation and measuring techniques for cold spot detection will support the targeted design and application of these new launcher concepts and solid state microwave components.

## CONCLUSION

Industrial systems for microwave pasteurization of packed, ready-to-eat food products, in particular, can provide for improved food safety and for both acceptable shelf life and high quality nutrition. New developments in microwave launchers and in microwave components based on solid state technology will facilitate the industrial application of these microwave driven industrial pasteurization systems.

## REFERENCES

[1] J. Tang, Unlocking Potentials of Microwaves for Food Safety and Quality, *Journal of Food Science*, vol. 80, no 8, pp. E1776-E1793, 2015.

# Comparison of High Power Magnetron and Solid State Microwave Sources for Compact Ultra High Q Applications

**John F Gerling**[1]

[1]Gerling Applied Engineering, Inc., Modesto, California, USA

**Keywords**: Magnetron, Solid State, High Power, High Q.

**Abstract:** High power CW (continuous wave) magnetrons are widely used as the source of energy in industrial microwave heating applications for their relatively low cost, high efficiency and good reliability. However, magnetrons may be undesirable for some applications, especially those having a high quality (Q) factor, due to performance limitations including frequency instability and wide spectral output. Solid state RF sources overcome some of these limitations by offering spectral purity and frequency agility. But while recent technological advances have greatly improved reliability and output power the comparatively higher cost of solid state RF sources limit their practicality for many applications. The choice between the two sources is further complicated by constraints relating to size and power coupling configurations. A recently completed experimental project involved a compact single-mode high Q microwave cavity having a loaded Q of approximately 7,000. The cavity was subject to slight shifts in resonance during operation, necessitating a microwave source having both narrow output spectrum and frequency agility in order to achieve efficient coupling. While output power in the range of a few tens of Watts was sufficient for this experiment, scale-up for practical implementation of the technology requires as much as 100 kW of microwave power and dc-RF conversion efficiency of at least 80%. Furthermore, an order of magnitude greater cavity Q would be required to achieve the desired system performance. Magnetron-based microwave sources meet the efficiency requirement, and those utilizing very low ripple power supplies have an output spectral bandwidth as low as 2 MHz, which is adequate for the < 3 dB bandwidth of the experimental cavity but not nearly adequate for scale-up. Solid state microwave sources typically have a much more narrow output bandwidth that is adequate for coupling to the scaled up cavity, although their dc-RF efficiency is lower and meeting the output power requirement is more costly and complex than magnetron sources. Finally, while a coaxial loop type coupler was suitable for launching into the experimental cavity, for scale-up the compactness of the cavity creates significant challenges to coupling at high power levels for both types of sources.

# Magnetic Characteristics of LTCC Ferrites Based Frequency Tunable Y-Junction Microstrip Circulator

**Punit Ravi Raj[1], Ananjan Basu[1]**

[1]Centre for Applied Research in Electronics, Indian Institute of Technology, Delhi, India

**Keywords**: LTCC ferrites, ferrite circulator, frequency tunable, self-biased.

## INTRODUCTION

A commercially available low-temperature co-fired ceramic (LTCC) ferrite tape ESL 40010/11 has been used in the design of a Y-junction circulator. Two designs with disk diameter × thickness of ∅6.9 × 0.539 mm and ∅3.9 × 0.62 mm have been fabricated to establish a relationship of applied magnetic field ($H_{appl}$), radius of ferrite disk ($R_{disk}$), and frequency of operation ($f_r$). Transmission parameters have been found in addition to the circulator frequency tunability by varying $H_{appl}$, thus providing a potential of designing self-biased frequency tunable circulators using LTCC process. They can be applied e.g. in multi-standard cellular systems, where miniaturized tunable RF front-end circuits realized in LTCC can be easily integrated with other RF components such as antennas, amplifiers, filters, etc. in System-in-Package (SiP) design. In radar and high-power microwave applications , the circulator can be used as a duplexer or an isolator.

## METHODOLOGY

Saturation Magnetisation ($4\pi M_s$), internal magnetic field $H_{in}$, and $R_{disk}$ are the key factors for ascertaining $f_r$ of the circulator. ESL 40010/11 ($4\pi M_s$ = 3800/3300 Gauss) [1], $H_{in}$ = 10 - 200 kA/m (out of plane direction), ferromagnetic resonance linewidth $\Delta H$ = 150 Oe, and tan $\delta_{\varepsilon,ferrite}$ = 0.04 were used for circulator design simulations. $R_{disk}$ of the ferrite disk resonator was further calculated by using formulae [2], [3], [4]

$$\mathbf{R} = \frac{1.84}{\mathbf{k}} = \frac{1.84}{\sqrt{\varepsilon_0 \varepsilon_r \mu_0 \mu_{eff}}} = \frac{1.84 \text{ x } c_0}{2\pi f \sqrt{\varepsilon_{r,ferrite}\, \mu_{eff,ferrite}}}$$

$$\mu = 1 + \frac{\omega_0 \omega_m}{(\omega_0^2 - \omega^2)}; \quad k = 1 + \frac{\omega \omega_m}{(\omega_0^2 - \omega^2)}; \quad \mu_{eff,ferrite} = \frac{\mu^2 - k^2}{\mu}$$

Simulations were undertaken for $H_{in}$ = 0 - 200 kA/m in ANSYS HFSS 14.0. The calculated width w of transmission line varies from 0.527 to 1 mm based on frequency of operation. By post-optimization, w = 0.8 mm was chosen to provide better matching with ferrite disk resonator. Simulation indicated that for $H_{in}$ = 119 kA/m, $R_{disk}$ = 3.45 mm, $f_r$ = 4 GHz, S21 = -1.23 dB, S12 = -25.95 dB, S11 = -18.74 dB. For $R_{disk}$ = 1.9 mm, $f_r$ = 5.4 GHz, S21 = -1.36 dB, S12 = -13.92 dB, S11 = -22.99 dB.

LTCC ferrite disk was fabricated by handcutting followed by pressure lamination (70 °C ) and low-temperature sintering (at 885 °C max temp) of tapes and silver conductor paste ESL 903-A. The backplane of circulator was fabricated on Rogers/RT Duroid 6010 ($\varepsilon_r$ = 10.2, h = 0.650 mm, tan δ = 0.0023). Permittivity $\varepsilon_r$ = 10.2 of the dielectric was chosen for continuous transition to magnetic boundaries of ferrite disk. A circular slot was cut into the dielectric for embedding sintered disk. Connections were made using silver-based epoxy conductor (Fig. 1). Permanent magnets of surface flux density $B_{appl}$ of 0.87 - 5.5 kG were used. $B_{appl}$ = 4.2 kG corresponds to $H_{in} \approx$ 119 kA/m, which is closer to saturation magnetization of ferrites used.

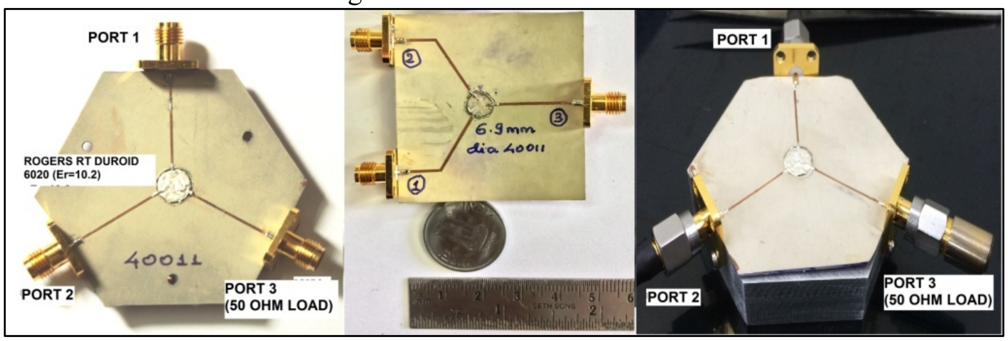


Figure 1. Fabricated Y-junction microstrip circulator

## RESULTS

$R_{disk}$ of the ferrite disk is reduced to increase $f_r$ of circulator keeping the $H_{appl}$ constant. Insertion Loss (IL) for a given $f_r$ reduces at fields closer to magnetization saturation. Beyond saturation $f_r$ increases due to a decrease in effective permeability $\mu_{eff,ferrite}$ (Table 1). Measured IL and isolation were found to be in close agreement with simulated results (Fig. 2). We also observed that increasing the $H_{in}$ beyond saturation gives the flexibility to tune circulator resonant frequency ($f_r$) as shown in Fig. 3.

Table 1. Measured results – $f_r$ and transmission characteristics vs $B_{appl}$.

| Applied Flux Density, $B_{appl}$ (kGauss) | $R_{disk}$ = 3.45 mm | | | | $R_{disk}$ = 1.9 mm | | | |
|---|---|---|---|---|---|---|---|---|
| | $f_r$ (GHz) | S21 (dB) | S12 (dB) | S11 (dB) | $f_r$ (GHz) | S21 (dB) | S12 (dB) | S11 (dB) |
| 0.87 | 4.4 | -8.68 | -20.63 | -12.622 | 5.84 | -6.48 | -13.32 | -11.59 |
| 2.7 | 3.94 | -4.38 | -14.35 | -12.96 | 5.5 | -4.49 | -14.48 | -21.63 |
| 3 | 4 | -4.9 | -14.03 | -18.38 | 5.5 | -4.06 | -17.35 | -21.71 |
| 3.3 | 4 | -4.43 | -18.53 | -17.5 | 5.5 | -3.69 | -15.79 | -28.41 |
| **4.2(~$M_s$) $H_{in}$ = 119 kA/m** | **3.98** | **-3.51** | **-18.65** | **-12.41** | **5.49** | **-2.37** | **-18.59** | **-** |
| 4.5 (>$M_s$) | - | - | - | - | 5.8 | -2.6 | -12.8 | -19.9 |
| 5.5 (>$M_s$) | 5.2 | -2.37 | -18.98 | -16.85 | 7.55 | -2.5 | -11.5 | -22.1 |

## DISCUSSION

Although conventional YIG and spinel ferrites provide better IL, LTCC ferrites provide freedom in the fabrication of planar SiP circuits, thus obviating the plumbing losses and reducing overall package area. Since $f_r$ can be tuned by $H_{appl}$, LTCC provides the possibility of self-biased circuits for the tunable circulator. Realization of integrated winding in ferrite LTCC (ESL 40012) to vary the internal magnetic field up to 0.4 T (saturation) using $H_{appl}$ < 2.5 kA/m has already been reported in [5]. Presently, our research is under progress for complete LTCC design wherein ESL 40010/11 ferrite tapes will be co-sintered with dielectric tape 41050 which can further incorporate integrated windings for a self-biasing circuit.

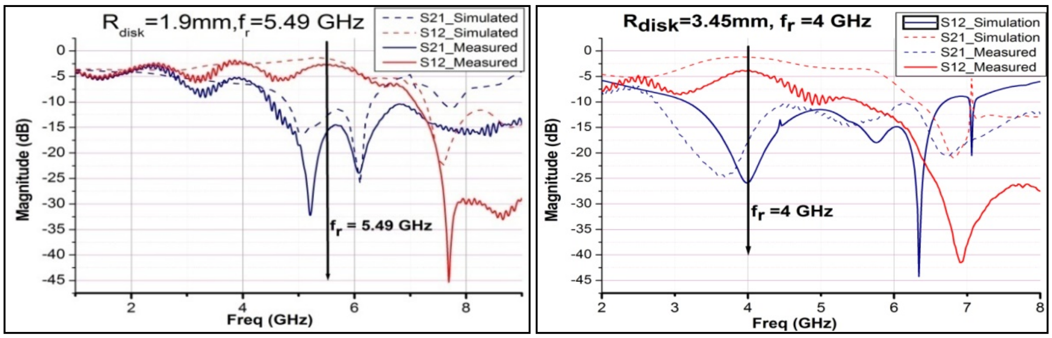


Figure 2. Simulated vs measured insertion loss (S21) and isolation (S12) for $H_{in}$ = 119 kA/m.

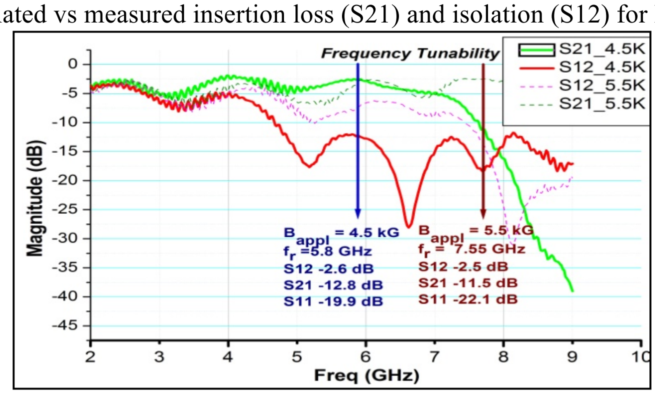


Figure 3. Frequency tuning of circulator by varying $H_{appl}$ (4.5 & 5.5 kG) for $R_{disk}$ = 1.9 mm.

## CONCLUSION

Y-junction microstrip circulator with $R_{disk}$ = 1.9 mm and 3.45 mm has been designed with parameters in close agreement with simulated results. Frequency tunability of the ferrite up to 130% has been demonstrated by varying $H_{appl}$ beyond saturation.

## REFERENCES


[1] W Zhang, M Mu, D Hou, Y Su, Q Li, and Fred C Lee, Characterization of LTCC Ferrite Laminates, *IEEE Transactions on Magnetics*, Vol. 49, No. 11, pp. 5454-5463, Nov 2013.

[2] H Bosma, On stripline Y-circulation at UHF, *Proceedings of IEEE - Part B: Electronic and Communication Engineering*, pp. 137-146, Jan 1962.

[3] J Helszajn (ed.), *Waveguide Junction Circulators - Theory and Practice*, Wiley, 1998.

[4] CE Fay and RL Comstock, Operation of the Ferrite Junction Circulator, *IEEE Transactions on Microwave Theory and Techniques*, vol. MTT-13, pp. 15-27, 1965.

[5] A Shamim, J Bray, N Hojjat, RA Elasoued, and D Baillargeat, Microwave and Magnetostatic Characterization of Ferrite LTCC for Tunable and Reconfigurable SiP Applications, *IEEE MTT-S International Microwave Symposium*, pp. 691-694, 2007.

[6] ESL Electro-Science data sheet: 40010/11, *www.electroscience.com/pdf/40010.pdf*.

# Development of Precise and Energy Saving Microwave Reactors with Solid State Microwave Source and Their Application to High Speed Synthesis of Valuable Functional Materials

**Takeko Matsumura [1] ,Kazunori Yamashita[1], Nobuo Mayama[2], Masateru . Nishioka[3] , Yuichi Utsumi[4], Akinobu Yamaguchi[4], Mitsuyoshi Kishihara[5]**

1. Minerva Light Laboratory, Kyoto, Japan.2. Chronix Co.Ltd, Tokyo, Japan.3. Aist, Sendai, Japan.4. University of Hyogo, Himeji Japan
5.Okayama Prefectural University, Okayama Japan

**Keywords**: solid state microwave generator, microwave synthesis, functional materials, phosphorescent metal complexes, nano materials

## INTRODUCTION

We studied various microwave reactors with solid state microwave generator and applied to microwave synthesis of functional materials such as luminescent metal complexes and metal nano particles.

Types of these microwave reactors are an elliptic type reactor(A), a flow type reactor with $TM_{010}$ mode(B), a coaxial flow reactor(C) and a resonance reactor(Ｄ) equipped with 2.45GHz microwave.(Figure 1)

In addition, a microchannel coupled with a post-wall 24.15 GHz wave guides(E) was developed and the on-chip synthesis of a ruthenium complex was performed.

## METHODOLOY

High speed and energy saving synthesis of valuable compounds such as phosphorescent metal complexes and nano materials are studied with these microwave reactors**.** Real time monitoring during microwave reaction are carried out with the elliptic microwave reactor (System A) and the flow type microwave reactor (System B) connecting with real time spectrometer with a fiber optic temperature sensor.

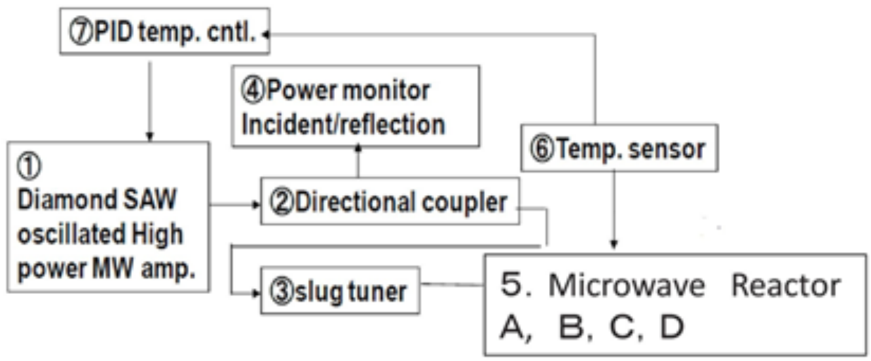


**Figure 1 System of microwave chemical reactor with solid state microwave generator**

## Result

With these microwave reactors, $Ru(bpy)_3^{2+}$ and their derivatives, synthesis of which need long time in conventional synthetic procedure, were synthesized in short time of 10 minutes. As for synthesis of Ir(III) complexes, the brightest phosphor for OLED, time required for synthesis was shortened from 20 hours to 20minutes.The experimental results for microwave synthesis of various functional materials by microwave reactors equipped with solid state microwave generators are described in detail.

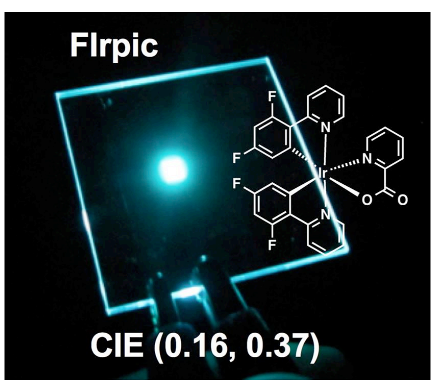


**Ir(F2ppy)2(pic) as dopant**

**Figure 3 Phosphorescent emitting feature of EL devices fabricated with MW synthesized highly pure Ir(III) cyclometalated complexes**

## CONCLUSION

Various types of microwave reactor with solid state microwave generators were developed and applied to rapid and precise synthesis of valuable functional materials.

## REFERENCES

T. Matsumura, T. Fujii, T. Fukuoka, E. Kurihara, T. Yajima, Chemical Engineering, 51(8),14-20(2006)

Y. Utsumi, A. Yamaguchi, T Matsumura-Inoue, M. Kishihara, On-chip synthesis of ruthenium complex by microwave-induced reaction in a microchannel coupled with post-wall waveguide, Sensors and Actuators B 242 (2017) 384–388

# A Software Intensive Architecture for Solid-State Microwave Generators

**Kenneth Kaplan**

Cellencor, Inc. Ankeny, Iowa, United States

**Keywords**: Solid state microwave, frequency agile SSPA, pulsed microwave, SSPA control software

## INTRODUCTION

The recent introduction of high-power solid-state microwave generators presents new capabilities not possible with magnetron-based microwave generators, including frequency agility, phase control, accurate output power control, and pulsed modulation mode. A robust and versatile new software control architecture using a graphical user interface (GUI) has been developed for industrial and scientific applications.

## HARDWARE ARCHITECTURAL OVERVIEW

The new National Electronics PrecisePower™ family of microwave generators operates in the ISM L band (902-928 MHz) and the ISM S band (2400-2500 MHz). The underlying hardware architecture is highly modular allowing generator configurations covering a wide range of power levels from one to75 kilowatts. Various sized systems are constructed from the required number of RF power modules. An intelligent RF exciter provides the RF drive to all the SSPA modules. It utilizes precision digital attenuators to provide a power control range of over 60 dB with better that 0.1% accuracy. It also provides a master RF oscillator output signal and an external RF input so multiple generators can be phase-locked or phase-shifted.

## SOFTWARE CAPABILITIES

The software requirements can be summarized as: a) fast and precise control of frequency, phase, and output power; b) real-time load monitoring and matching to maximize power transfer and to protect the system; c) provide a versatile and easy to use user interface; and d) provide easy interfacing to external hardware and software for remote control. In this architecture all real-time control functions are performed locally in functional hardware modules by multiple embedded microcontrollers linked by a high speed local data bus. The exciter and power modules utilize fast, high accuracy, and wide dynamic range RF detectors to measure forward and reflected power at the module and system levels. The microcontrollers also read numerous other precision sensors to monitor temperatures, currents, and voltages.

The main control program typically runs on a standard Windows-based PC which is connected to the solid-state generator via a USB 2.0 connection. The GUI provides full control and monitoring of the system. The main screen (Fig. 1) has buttons and numeric indications to set and monitor key operating parameters such as frequency, power, and modulation. The central part of the main screen is a band-map graph. The X axis represents frequencies across the entire band. Plot lines show operating frequency boundaries, preset and actual output power levels, and reflected power readings and limits. Band-map presets can be saved or loaded from saved files.

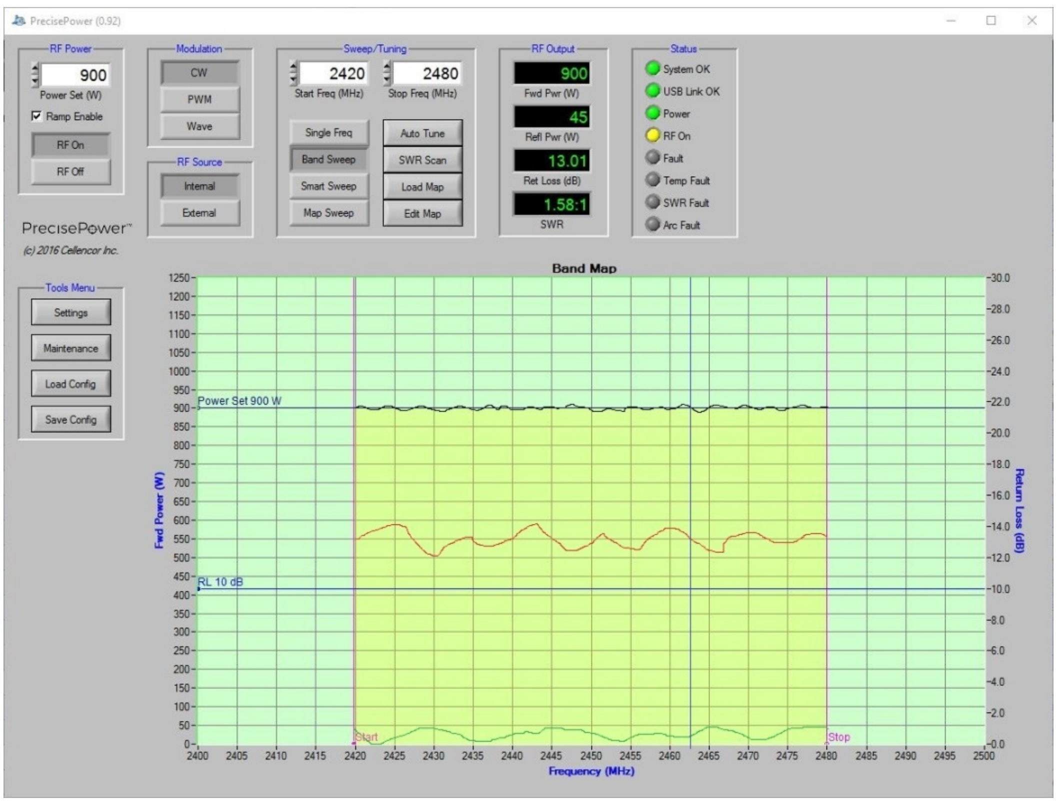

Figure 1. PrecisePower™ Main User Interface Screen

A critical issue in high-power microwave applications is matching the generator output and transmission line impedances to the load impedance. Real world loads are seldom well matched and or stable due to changes over time of workload material composition, temperature, moisture content, etc. This is typically of single frequency magnetrons which can result in high levels of reflected power. Waveguide tuners can be used to improve the match but are slow and expensive. Since solid-state generators are frequency agile, load impedance matching can often be accomplished by tuning the generator to an optimal frequency or set of frequencies. The system has an automatic tuning function which scans across the entire band to identify the optimally matched frequencies, and plots them on the band map. Depending on the characteristics of the load, the best single frequency can be used, or the system can frequency sweep or hop within favorable band segments. Automatic matching can operate continuously while the system is producing full power.

A related function optimizes the distribution of energy using frequency sweeping in a microwave applicator (cavity, oven, etc.) which vary in size and shape. At any given frequency, an applicator will have "hot" and "cold" spots due to constructive and destructive interference of waves within it, often requiring mechanical devices to stir the waves or move the load. Changing the operating frequency causes the power nodes and antinodes to move around considerably, so frequency sweeping across the band can optimize spatial energy distribution (Figure 2). The software supports various configurable automatic frequency sweeping modes.

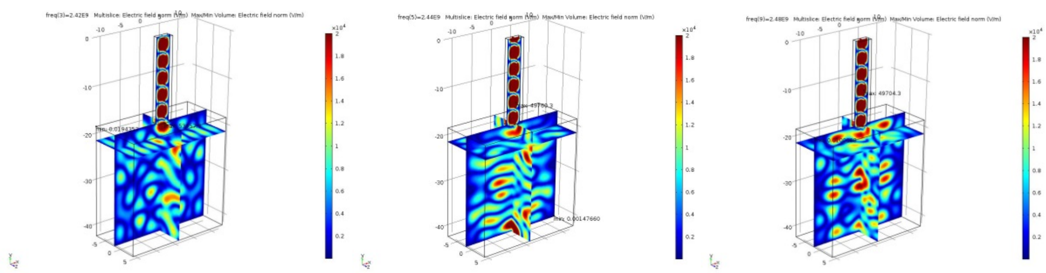

Figure 2. Electromagnetic simulation of top waveguide fed loaded rectangular cavity at 2420 MHz, 2440 MHz, and 2460 MHz respectively.

The software also provides functions for remote control, either basic power control using PLC-style hardwired signals, or internet based advanced software control using LabView™.

## CONCLUSION

Solid-state microwave generators offer important new capabilities and features. A robust and easy to use software control system can significantly enhance utilization of these capabilities in real-world industrial or scientific applications.

## REFERENCES

Bows JR, **Variable Frequency Microwave Heating of Food**, JMPEE, Vol 34 No 4, 1999

Luan D, Wang Y, et al, **Frequency Distribution in Domestic Microwave Ovens and Its Influence on Heating Pattern**, Journal of Food Science, 2016

Lee HS, Choi, JJ, Cho, GS, **Microwave plasma sources by using pulse mode SSPA** 2014 IEEE 41st International Conference on Plasma Sciences (ICOPS) held with 2014 IEEE International Conference on High-Power Particle Beams, 25 May 2014

 

# Numerical Simulation of the Electric Field and Temperature Distribution within a Low Loss Material in a Travelling Wave Applicator

**Candice Ellison[1] and Dorin Boldor[1,2]**

[1]Louisiana State University, Baton Rouge, LA, U.S.A.
[2]LSU AgCenter, Baton Rouge, LA, U.S.A.

**Keywords**: Finite element modeling, electrical field distribution, temperature profile, standing wave, travelling wave.

## INTRODUCTION

Microwave heating applications often require uniform temperature distribution throughout the processed material; however, hot spots and thermal runaway limit the temperature uniformity primarily due to standing waves and decay of microwaves. The design of microwave applicators as well as the physical characteristics of the material to be heated are crucial for efficient delivery of microwave energy to the workload at the operating frequency. Many means of attaining uniform material heating in microwave applicators have been proposed in the literature including turntables, mode stirrers, sliding shorts, variable frequency, and constant sample movement. While these solutions have merit in many applications, these are not easily implemented in a single mode travelling wave applicator. Another approach to designing microwave systems with the desired (e.g. uniform) heating profile is via material design optimization. Studies have been published on attaining uniform heating distribution in low loss materials by means of dielectric Cantor multilayers, controlling composite structures, and other material optimization in travelling wave applicators [1, 2]. The current study presents a numerical simulation using finite element modeling of the electrical field distribution in a rectangular waveguide at 2.45 GHz as well as the heating distribution in a low loss load placed at the center of the waveguide to gain a better understanding of the heating characteristics of the sample material.

## METHODOLOY

Finite element methodology (FEM) was used to model the electric field and temperature distribution of the sample material during microwave irradiation in a travelling waveguide by using COMSOL Multiphysics software. A modified WR430 waveguide (to account for the presence of the dielectric) in the $TE_{10}$ mode was modeled with the sample material placed at the center of the waveguide. Measured and calculated material properties were input for the sample material, pine sawdust, which is used as an example of a low loss dielectric. A 600W power source of 2.45 GHz was placed at one end of the waveguide. The model was solved using two different boundary conditions placed on the exit port: perfect electric conductor and scattering boundary condition. By changing the boundary conditions at the exit port, both a standing wave and a travelling wave were simulated for comparison. Assuming no losses on the waveguide walls, Maxwell's equations were solved for the air and material domains and the heat transfer equation was solved for the material domain.

To verify the model, experimental runs were conducted in which a quartz U-tube was loaded with 20 g pine sawdust and placed in a travelling wave applicator. The sample was irradiated with 2.45 GHz, 600 W microwave power and the temperature distribution was recorded by an infrared camera.

**RESULTS**

The resulting electric field from the model confirms a standing wave pattern when a reflective boundary condition is set at the end of the waveguide (Figure 1). In the travelling wave configuration (Figure 2), resulting from a scattering boundary condition at the end of the waveguide, the intensity of the electric field decays after it passes through the material. For the standing wave simulation, the heating profile of the material consists of alternating hot and cold spots that are at ¼ wavelength intervals across the heated material (Figure 3a). The temperature profile resulting from the travelling wave simulation (Figure 3b) is more uniform compared to the standing wave configuration as the crests of the waves in this conformation appear to move across the material. Figure 4 depicts the hot and cold spots manifested in charred and not charred regions after experimental microwave treatment of sawdust in a standing wave microwave configuration.

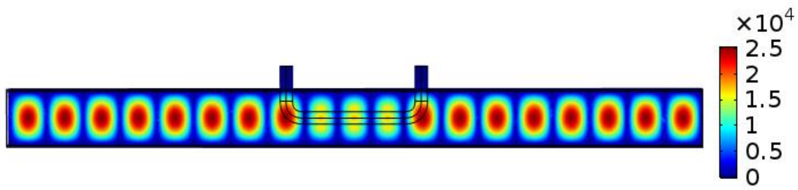


Figure 1. Simulated electric field (V/m) resulting from 2.45 GHz microwave irradiation at 600W for astanding wave configuration

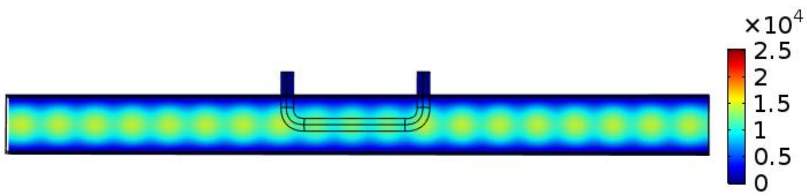


Figure 2. Simulated electric field (V/m) resulting from 2.45 GHz microwave irradiation at 600W for a travelling wave configuration

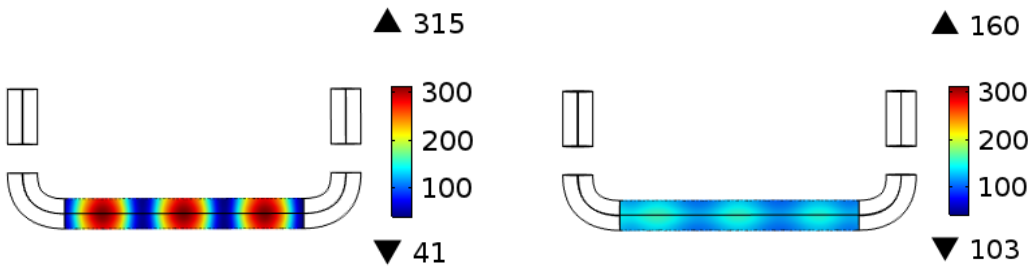


Figure 3. Simulated temperature profile (in °C) after 1 minute of microwave irradiation at 600W and 2.45 GHz for (a) standing wave and (b) travelling wave configurations.

Figure 4. Charred and not charred regions in pine sawdust sample after microwave treatment.

## DISCUSSION

The model shows good agreement with experimental studies in which an infrared camera was used to observe the heating profile of the sample material, dry woody biomass, during microwave irradiation. Further, the simulated electric field distributions are consistent with similar studies found in the literature [3]. Future studies will focus on optimization of temperature uniformity by implementation of a sliding short. The dielectric and thermal properties of the material under test are well defined through measurements of dielectric properties and thermal conductivity.

## CONCLUSION

The presented numerical model improves our understanding of the heating characteristics of the sample material in a travelling wave applicator. This will provide a basis for future studies in which a sliding short will be implemented to optimize the uniformity of the temperature profile. A continuous sliding short will effectively change the phase of a standing wave with time so that the regions of high intensity electric field will vary across the material with time and help maximize energy transfer to the load.

## REFERENCES

[1] K.A. Lurie and V.V. Yakovlev, Method of control and optimization of microwave heating in waveguide systems, IEEE Trans. Magn, vol. 3, p 1777, 1999.

[2] F. Chiadini, A. Diovisalvi, V. Fiumara, and A. Scaglione, A Cantor multilayer traveling wave applicator for microwave heating: Numerical analysis and design, J. Appl. Phys., vol. 116, no. 21, p. 214503-1-214503-9, 2014.

[3] E.M. Moon, C. Yang, and V.V. Yakovlev, Microwave-induced temperature fields in cylindrical samples of graphite powder – experimental and modeling studies, Intern. J. Heat & Mass Transfer, vol. 87, no 8, pp. 359-368, 2015.

# Application of Radio Frequency Drying on Soybean Residue

**Yu-Fen Yen, Su-Der Chen***

National Ilan University, I-Lan City, Taiwan 26047

**Keywords**: radio frequency (RF), drying, soybean residue, quality.

## INTRODUCTION

The soaking soybean can be squeezed to soybean milk and soybean residue. The soybean residue still contains a lot of nutrients and is suitable for animal feed [1]. However, a mass of soybean residue has high moisture content and needs to dry for industrial application. Although soybean residue can be dried by hot air drying, but it requires long time to accomplish due to heat transfer resistance. Radio frequency processing (RF) is the use of rapid alternating electric field technology, then rotational vibration of the polar water molecules and rapid movement of ions cause friction and heat in the sample. [2] Therefore, RF-cold air drying can significantly reduce drying time and energy consumption than conventional hot air drying. Moreover, soybean residue from soybean milk still has high total polyphenols content and scavenging effect of DPPH free radicals, which may be affected by different drying method. [3] Therefore, RF-cold air drying could be suitable application for soybean residues in industry.

## METHODOLOY

A 5 kW, 40.68 MHz pilot-scale RF with cold air drying system was used in this study. The size of the parallel electrode plates were 35 cm x 35 cm. The soybean residue was placed in a PP plastics bucket and put on the bottom of RF electrode plate. The RF power was obtained by adjusting the gap between the electrodes from 10 to 22 cm. The surface temperature profiles of 1.5 kg soybean residues after RF-cold air drying were measured by IR sensor at three different locations. Moreover, the weight loss of soybean residue was determined at different time interval to obtain the drying rate and drying curve.

## RESULTS

The RF-cold air drying of soybean residues required only 22 min to accomplish drying processing, compared with 330 min cold air drying. (Fig. 1) The final temperature and moisture content of soybean residues by RF-CA drying were 88℃ and 0.12 kg water/ kg dried material, respectively. (Fig. 2) RF-cold air drying can significantly reduce drying time and energy consumption (Table 1).

Fig. 1. Drying curves of soybean residues by cold air (CA) and RF-cold air drying (RF-CA).

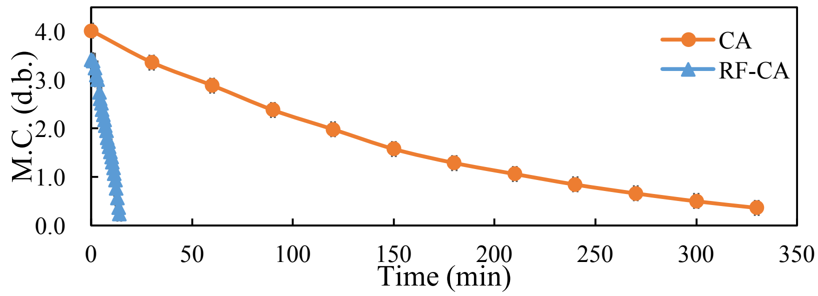


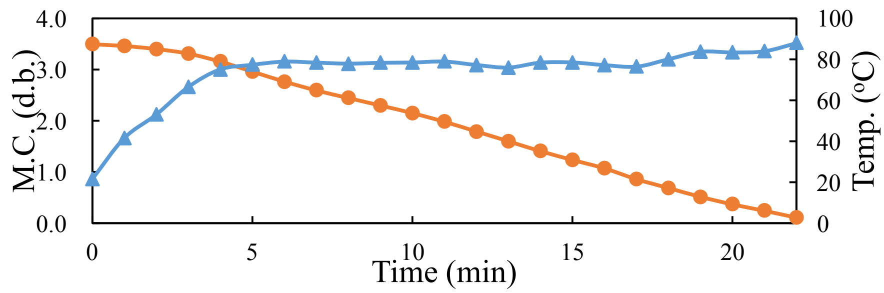


Fig. 2. The drying curve and temperature profile of 1.5 kg soybean residue by RF-CA drying.

Table 1. The drying rate, drying time and energy consumption of drying soybean residue

| Drying conditions | Drying rate (g/min) | Drying time (min) | Total energy (kW) |
|---|---|---|---|
| RF-cold air drying | 52.3 | 22 | 2.31 |
| Cold air drying | 2.14 | 330 | 13.53 |

## DISCUSSION

The drying rate of soybean residues was 52.3 g/min, and it only took 22 min to accomplish by RF-CA drying.

## CONCLUSION

RF-cold air drying is very suitable application for soybean residues in food industry due to shorter drying time, faster drying rate and less energy consumption.

## REFERENCES

[1] W.C. Vong, S.Q. Liu, Biovalorisation of okara (soybean residue) for food and nutrition, *Trends Food Sci Technol.*, vol. 52 , pp.139-147, 2016.
[2] Z. Huang, B. Zhang, F. Marra and S. Wang, Computational modelling of the impact of polystyrene containers on radio frequency heating uniformity improvement for dried soybeans, *Innov Food Sci Emerg*., vol. 33, pp.365-380, 2016.
[3] M.M. Muliterno, D. Rodrigues, F.S. de Lima, E.I. Ida and L.E. Kurozawa, Conversion/ degradation of isoflavones and color alterations during the drying of okara. *LWT - Food Sci Technol.*, vol. 75 pp.512-517, 2017.

# Microwave Modelling Applied at Continuous In-flow Microwave Preservation of Foods and Combined Microwave Bread Baking

**B. Wäppling Raaholt**[1]

[1]RISE Research Institutes of Sweden, Göteborg, Sweden; Birgitta.Raaholt@ri.se

**Keywords**: microwave modelling, electromagnetics, microwave processing, baking, electromagnetic modelling, food applications

## INTRODUCTION

In this presentation, examples of microwave modelling will be given for continuous in-flow microwave preservation as well as for combined microwave baking.

Tubular microwave processing of pumpable particulate foods offers an alternative way to produce high-quality shelf-stable foods. The system is implemented at RISE [1], pressurized and equipped with a robust control system to facilitate microwave heat treatment of particulate foods at temperatures up to 140 degrees centigrade (284°F). The microwave heating part of the system includes two types of cavities, each of them with appropriately selected microwave modes. These contribute to a more uniform microwave heating over the cross-section of the tube.

A simplified model for microwave heating of pumpable, semi-viscous foods in a tubular system will be presented and illustrated. The model incorporates an assumed velocity profile as well as radial heat transfer. Moreover, measurements in a continuous in-flow microwave processing system developed in pilot-scale for particulate as well as homogeneous foods will be exemplified. Results from implementing an extended multi-physics model will also be illustrated and discussed.

Moreover, use of modelling will be visualized for the application of combined microwave baking of bread [2]. Industrial baking of bread is one of the most energy-requiring processes in food industry. Available data on energy demand for industrial baking processes vary considerably with factors such as energy source, type of oven (continuous ovens or batch-wise ones, etc.), and type of bread to be baked. Target temperature and baking time often vary considerably with bread type, mass of each dough item etc. Modelling of baking as well as post-drying processes often offers valuable tools for process optimization, with resulting process designs which corresponds to reduced energy use while maintaining bread quality. Furthermore, modelling enables a time-efficient means of feasibility studies, in terms of up-scaling to industrial scale.

A mathematical model of baking will be illustrated to describe the mechanisms occurring within the bread during baking. The model could be used to exemplify how changes in process conditions may affect the physical phenomena in bread during baking, which in turn is directly related to control of product quality. Reduced energy consumption and baking time will be exemplified and compared to conventional baking.

## METHODOLOY

Continuous in-flow microwave processing of pumpable foods was modelled by combining a radial model for microwave heating with a flow profile model for a semi-viscous, pumpable food system at 2450 MHz. The food studied was a model product, used to model soup or sauce. The resulting achieved temperature distribution will be exemplified and discussed in terms of measurements in a pilot-scale system.

Furthermore, results from implementing a multi-physics model of tubular microwave heating of homogeneous foods will be exemplified and presented.

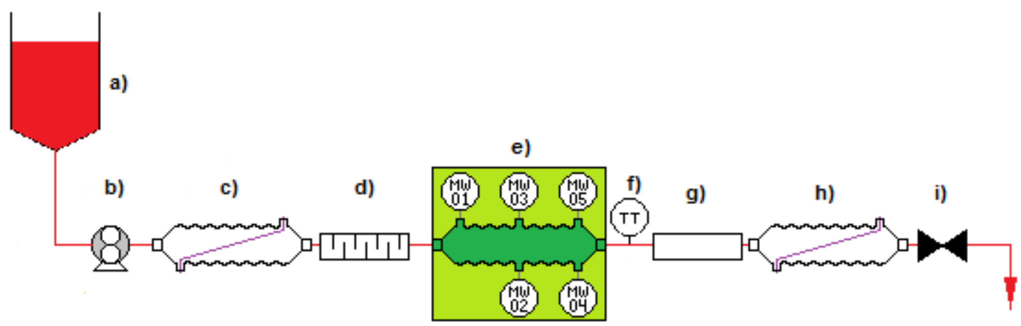


(a) (b)

Figure 1. Schematic diagram of the microwave processing system, including: balance tank (a), product pump, (b), pre-heater (c), static mixer (d), microwave heating unit (e), spatial temperature measurement unit (f), holding tube (g), cooler (h) and pressure regulator (i).

Calculations of a processing line for microwave baking of a bakery product, followed by convective post-drying, will be described in terms of energy reduction and reduced processing time. Comparisons will be made to a corresponding conventional line for baking and drying.

## RESULTS AND DISCUSSION

For continuous in-flow microwave processing, modelling combined with measurements were used to find an appropriate combination of microwave power levels at each of the cavities, resulting in a more levelled out microwave heating over the tubular cross-section. The results exemplify the use of microwave modelling as a powerful tool to design and optimize microwave systems.

Results from microwave baking of a bakery product, followed by convective post-drying, will be described in terms of energy reduction and reduced processing time. For a baking application the resulting energy use could be significantly reduced, as will be illustrated at the conference by modelling results for a selected process.

## CONCLUSIONS

Continuous in-flow microwave processing offers means of heating foods more uniformly over the cross section, resulting in an alternative way to produce high-quality foods.

Combined microwave baking of bread offers an energy-efficient way to produce high-quality bread.

## REFERENCES

1. **B. Wäppling Raaholt, S. Isaksson, L. Hamberg, A. Fhager, and Y. Hamnerius, Continuous tubular microwave heating of homogeneous foods: evaluation of heating uniformity, *Journal of Microwave Power and Electromagnetic Energy*, Vol. 50 (1), p. 43-65, 2016.**
2. **B. Wäppling Raaholt, "Application of microwave processing of foods", SP report 2015:38, ISSN 0284-5172.**

# Radio Frequency (RF) Thawing of Irregular Shape Frozen Beef —A Computational Simulation and Study

**Yulin Li[1], Yifen Wang[1,2] and Yang Jiao[1,*]**

[1]Shanghai Ocean University, Shanghai, China
[2]Auburn University, Auburn, USA

**Keywords**: Radio frequency, thawing, irregular shape, heating uniformity

## INTRODUCTION

Radio frequency (RF) thawing can reduce processing time, minimize nutritional damage, and also improve thawed product quality. Because of its large penetration depth and high heating rate, RF thawing has great potential for rapid thawing and improve heating uniformity. Thawing is a process that requires heat and involves phase changes, which make the process complicated [1]. Although there are studies explore the influencing factors of RF heating [2-4], not much has been studies on RF defrosting and its related influencing factors and various behavior of samples processed in industrial RF thawing lines. Some industrial radio frequency heaters are developed and applied in fish/meat block thawing [5-6], but these majorly work well with regular shape frozen products. Beef carcasses are usually cut into halves or quarters before freezing, which are in irregular shape. More information is needed to understand how and how much would shape influence the heating behavior of frozen materials in RF thawing. The purpose of this study was to develop a mathematical model of RF thawing of irregular-shape frozen beef, explore the internal temperature distribution of the irregular beef during RF thawing, and then to study the influence of thickness, shape, volume and other factors on the uniformity of the thawing of beef.

## METHODOLOY

COMSOL Multiphysics® was used to simulate the thawing process by entering the physical properties of frozen beef samples including dielectric properties, thermal characteristics change with temperature to the software. Sample properties and simulation details are listed below.

Then the internal temperature change and distribution was calculated. Using computers to simulate three different thickness of beef (17.2×12×3.8cm; 17.2×12×5.8cm; 17.2×12×1.8cm); three different volumes of beef (17.2×12×3.8cm; 24.3×17×3.8cm; 34.4×24×3.8cm); three different surface shapes of beef (rectangle; steps; trapezoid) (Fig. 1). Beef thawing were simulated in a 27.12 MHz frequency RF system from -13ºC to 4ºC.

**Table 1. Parameters, initial and boundary conditions for solving COMSOL model*)**

<table>
<tr><td>Sample initial temperature</td><td colspan="3">-13 [degC]</td></tr>
<tr><td>Sample density</td><td colspan="3">T<Tm1, $\rho$=961 [kg/m$^3$]<br>Tm1<=T<=Tm2, $\rho$=1007 [kg/m$^3$]<br>T>Tm2, $\rho$=1053 [kg/m$^3$]</td></tr>
<tr><td>Sample specific heat</td><td colspan="3">T<Tm1, $c_p$=1935.2 [J/(kg degC)]<br>Tm1<=T<=Tm2, $c_p$=153016.3 [J/(kg degC)]<br>T>Tm2, $c_p$=153016.3 [J/(kg degC)]</td></tr>
<tr><td rowspan="13">Sample dielectric properties</td><td>Temperature [degC]</td><td>Dielectric constant</td><td>Dielectric loss factor</td></tr>
<tr><td>-18</td><td>2</td><td>2</td></tr>
<tr><td>-15</td><td>9</td><td>9</td></tr>
<tr><td>-10</td><td>22</td><td>35</td></tr>
<tr><td>-5</td><td>48</td><td>108</td></tr>
<tr><td>-3</td><td>79</td><td>175</td></tr>
<tr><td>-1</td><td>83</td><td>268</td></tr>
<tr><td>0</td><td>84</td><td>270</td></tr>
<tr><td>1</td><td>85</td><td>284</td></tr>
<tr><td>3</td><td>87</td><td>286</td></tr>
<tr><td>5</td><td>88</td><td>290</td></tr>
<tr><td>10</td><td>91</td><td>318</td></tr>
<tr><td>15</td><td>90</td><td>374</td></tr>
<tr><td>Convective heat transfer coefficient</td><td colspan="3">10 [W/m$^2$*K]</td></tr>
<tr><td>Working frequency</td><td colspan="3">27.12 [MHz]</td></tr>
<tr><td>Electrode voltage</td><td colspan="3">1375 [V]</td></tr>
<tr><td>Electrode gap</td><td colspan="3">12 [cm]</td></tr>
<tr><td>Surrounding temperature</td><td colspan="3">20 [degC]</td></tr>
<tr><td>Heating time</td><td colspan="3">6000 [s]</td></tr>
</table>

*) Dielectric properties were measured in this work, all the other properties obtained from [7].

After 6000s RF thawing under a voltage of 8000 V, thawing rate and temperature uniformity of different thickness, different volumes, and different shapes were compared. Temperature uniformity index (UI) is used to evaluate the heating uniformity [7].

$$TUI = \frac{\int_{V_{vol}} |T - T_t| dV_{vol}}{(T_t - T_{initial}) V_{vol}} \quad (1)$$

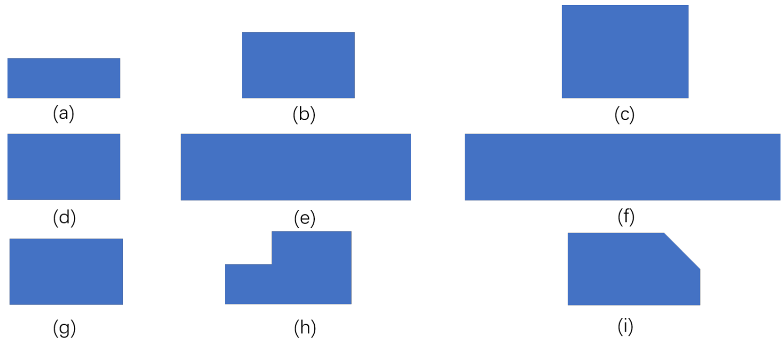


Figure 1. Scheme of frozen beef sample with different thicknesses (a,b,c), surface areas (d,e,f), and shapes (g,h,i). (Dimensions shown in text above)

where $T$ is the local temperature in the food (ºC), $T_{initial}$ is the initial temperature of the food (ºC), $T_{ave}$ is the average temperature of the volume (ºC), $V_{vol}$ is the volume of food ($m^3$), and $T_t$ is the target heating temperature (ºC). A smaller index corresponds to better heating uniformity.

## RESULTS

Temperature distribution of thawed beef samples are shown in Figure 2. Results show that thawing rate decreases as thickness increases. Accordingly, the temperature uniformity index (UI) increases from 0.0023950 to 0.0025876 and 0.0026159 when thickness increased from 1.8 to 3.8 and 5.8 cm. When expanding the volumes of beef, the original size beef is the first to reach to -4ºC with the lowest UI, then comes the 4 times and 9 times volumes. When thawing different shapes of beef, the step shape has the highest heating rate, the trapezoid is the second and finally comes the rectangle. The UI of rectangle, step shape, trapezoid are 0.002395, 0.002302, and 0.002175, respectively (Table 2).

## DISCUSSION

The simulation results show that the internal temperature distribution changed significantly with geometrical factors. When the other conditions are constant, the temperature of smaller size beef rises faster. Also, when the surface areas increased, the temperature uniformity decreased.

## CONCLUSION

All the factors including thickness, surface area (volume), and shapes influenced the heating behaviors significantly, which should be paid more attention when designing a versatile industrial RF thawing line of frozen beef with various sizes. On edge heating aspects, thicker materials have relatively severe edge heating problems, and irregular shape samples with sharp edges results in much higher temperature than those with regular shapes. In further research, a quantitative analysis should be performed on the influence of each factor. The results can be applied to explore the spot of the sample that might have the most severe quality degradation.

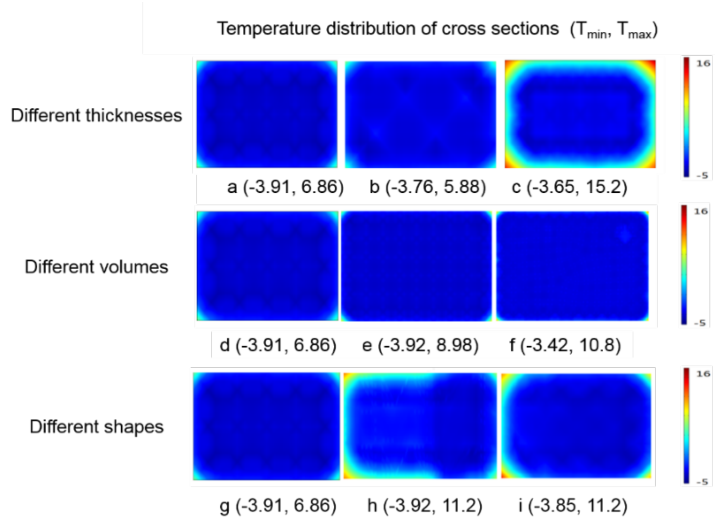


Figure 2. Temperature distribution of a cross-sectional surface of frozen beef with various thicknesses, volumes and shapes.

**Table 2. Heating uniformity index (UI) of the thawed beef with various thickness, volumes and shapes.**

| | Uniformity index (UI) | | |
|---|---|---|---|
| **Different thicknesses** | a<br>0.0023950 | b<br>0.0025876 | c<br>0.0026159 |
| **Different volumes** | d<br>0.0023950 | e<br>0.0052197 | f<br>0.01174 |
| **Different shapes** | g<br>0.0023950 | h<br>0.0023023 | i<br>0.0021753 |

## REFERENCES


[1] Y. Llave, S. Liu, M Fukuoka, et al. Computer simulation of radiofrequency defrosting of frozen foods, *J. Food Eng.*, *152(C)*, 32-42, 2015.

[2] G. Tiwari, S. Wang, J. Tang, S.L. Birla, Analysis of radio frequency (RF) power distribution in dry food materials, *J. Food Eng.*, *104*, 548-556, 2011.

[3] Uyar, R., Erdogdu, F., Sarghini, F., & Marra, F. Computer simulation of radio-frequency heating applied to block-shaped foods: Analysis on the role of geometrical parameters, *Food and Bioproducts Processing, 98*, 310-319, 2016.

[4] Chen, L., Huang, Z., Wang, K., Li, W., & Wang, S. Simulation and validation of radio frequency heating with conveyor movement, *J. Electromagnetic Waves and Applications, 30*(4), 473-491, 2016.

[5] Sanders, H. R. Dielectric thawing of meat and meat products, *J of Food Tech, 1*, 183–192, 1966.

[6] Jason, A. C., & Sanders, H. R. Dielectric thawing of fish, *Food Tech, 16*(6), 101–112, 1962.

[7] Jiao, Y., Shi, H. J., Tang, J. M., Li, F., & Wang, S. J., Improvement of radio frequency (RF) heating uniformity on low moisture foods with Polyetherimide (PEI) blocks, *Food Res. Intl, 74*, 106-114, 2015.

[8] Uyar, R., Bedane, T. F., Erdogdu, F., Palazoglu, T. K., Farag, K. W., & Marra, F. Radio-frequency thawing of food products - a computational study, *J. Food Eng, 146*, 163-171, 2015.

# Development of an Advanced Microwave Calorimeter for Monitoring of Chemical Reactions

**V. Ramopoulos[1], S. Soldatov[1], M. Hetz[1], G. Link[1] and J. Jelonnek[1,2]**

[1] IHM, Karlsruhe Institute of Technology, 76344 Eggenstein-Leopoldshafen, Germany
[2]IHE, Karlsruhe Institute of Technology, 76131 Karlsruhe, Germany.

**Keywords**: microwave heating, calorimetric measurements, liquids.

## INTRODUCTION

Microwave chemistry shows increasing application in last years. Owing to selective and volumetric nature of microwave heating it enables a faster and more energy efficient reaction [1]. For the successful design of microwave applicators, beside the knowledge on dielectric properties the detailed knowledge on the reaction kinetic and power requirements is important. If the chemical reaction is accompanied with a heat transfer, the calorimetry is a powerful method for reaction kinetics investigation. Of course such a calorimetry implies the in-situ measurement of temperature and the heat transfer rate to the reactive materials. To define a full balance of microwave and heat energy in the system both the incident reflected and absorbed microwave powers as well as the temperature of all components in the system need to be controlled. Calorimetric measurement were reported in [2, 3] for cylindrical cavity systems with a high quality factor, where the incident and reflected powers were estimated in the measurement cell. However, only qualitative calorimetric measurements had been feasible. In the present work the microwave measurements were extended with multi-physics simulations to enable a more quantitative estimation of the absorbed power in the material under test.

## METHODOLOY

A $TM_{010}$ mode cylindrical cavity, 88 mm in diameter and length of 88 mm, was used, which operates at around 2.45 GHz and has a quality factor of about 8000 and a transmission $S_{21}$ from -45 dB. This cavity, typically used for dielectric measurements, was improved for simultaneous calorimetric measurements. As a heat source a high power microwave amplifier (WMP2350/700/50MK-A) driven by a network analyzer (VNA) was used. The output power of the amplifier is fed into the measurement cavity. An Anritsu ML2488B power meter is used to measure incident and reflected power. The isolation of the incident and reflected signals is realized by using a waveguide circulator and a waveguide directional coupler. For accurate power measurements the VNA and the power meter need to be perfectly synchronized. The sample temperature has been measured using a fiber-optic sensor (TSNano from Optocon). The temperature of the cavity walls was kept constant at 15 °C to avoid minor changes in the cavity geometry and electric conductivity. The overall structure of the measurement system is shown in

Fig. 1. For estimating the sample specific heat the total power absorbed $P_{abs}$ in the cavity and the corresponding temperature increase at a heating rate of 5 K/min. were measured. To specify that part of $P_{abs}$, responsible for the measured sample temperature increase, CST Microwave Studio® was employed. To further improve the accuracy, the heat transfer losses from the sample were simulated with COMSOL Multiphysics®.

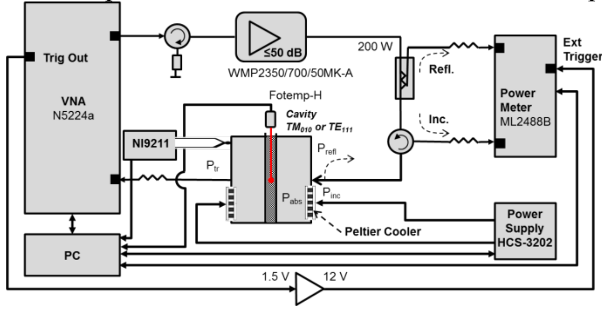


Figure 1 Block diagram of the designed system

## RESULTS

To validate the accuracy of the developed microwave calorimeter in absolute values, the heat capacity $c_p$ of two well-known liquids was measured and compared against literature values. Although calorimetric measurement is hardly feasible in a system where a sample never is in thermodynamic equilibrium with its environment, the measured data is already at the same order of magnitude, as can be seen from the following table. The estimate errors based on mentioned CST and COMSOL simulations as well as on residual errors in the measurement network calibration of about 0.01 dB are still too small. Further system optimization based on changes in the coupling design, sample size and heating rate are still going on. The final optimized concepts will be presented at the conference.

Table 1 Comparison of specific heat capacity measured with those in the literature

| **Material** | **$c_p$ (literature)** | **$c_p$ (measured)** |
|---|---|---|
| **Ethanol** | 2.4 J/(g*K) | 3.9 ± 0.5 J/(g*K) |
| **Ethylene glycol** | 2.2 J/(g*K) | 3.6 ± 0.4 J/(g*K) |

## ACKNOWLEDGMENT

This project has received funding from the European Union's Horizon 2020-SPIRE-2015 research and innovation programme under grant agreement No 680426, SYMBIOPTIMA. This paper reflects only the author's view. The Commission is not responsible for any use that may be made of the information it contains.

## REFERENCES


[1] L. Zong et al., Journal of Microwave Power and Electromagnetic Energy, vol. 38, no. 1 (2003), 49-74.

[2] A. Nesbitt, et al., Meas. Sci. Technol.; vol. 15 (2004) 2313–2324.

[3] J. M. Catala-Civera, et al., IEEE Transactions on Microwave Theory and Techniques, vol. 63, no. 9 (2015), 2905-2914.

# PtCo Electrocatalyst Prepared by Microwave–Assisted Polyol Modified Method for the Oxygen Reduction Reaction

**M.A. García-Contreras[1*], M. González-Muñoz[1,2]**

1Instituto Nacional de Investigaciones Nucleares, Carr. Mex-Tol s/n Ocoyoacac, Edo. Mex. C.P: 052750, Mexico

2Universidad Politécnica del Valle de Toluca, Carr. Toluca-Almoloya de Júarez Km. 5.6 Santiaguito Tlalcilalcali, Almoloya de Júarez, Edo. Méx. C.P. 50904, Mexico

**Keywords**: Electrocatalyst, platinum, cobalt, microwaves, polyol method.

## INTRODUCTION

Fuel cells are devices that convert chemical energy into electrical energy. In a fuel cell, the chemical energy is supplied by a fuel and an oxidant that are stored outside the cell and the electrochemical reactions are carried out inside. Low temperature fuel cells require electrocatalysts to accelerate cathodic and anodic reactions, oxygen reduction (ORR) and hydrogen oxidation, respectively. In a fuel cell, the cathodic reaction, ORR, is very important because of the energy consumption involved, about four times the anodic reaction, hydrogen oxidation. The ORR is slow kinetically, which is a very important parameter in the performance of the fuel cells. Fuel cells operate with high efficiency and very low levels of contamination [1]. Currently, platinum is the leading metal as an electrocatalyst for ORR, but because of its high cost and low relative abundance, great efforts have been made in the last decades to replace it as much as possible and a variety of electrocatalysts have been tested with relatively acceptable results. In recent years interest has arisen to investigate nanocrystals with core-shell architecture due to their better catalytic, optical, magnetic and electrical properties. Among the combinations studied, those that consist of a low-cost metal in the core of the electrocatalyst and a noble shell metal have received special attention due to the functional and economic advantages they present [2]. A catalyst with a very thin coat of a noble metal over a transition metal in the center not only reduces the required amount of noble metal, but could significantly increase its catalytic properties by means of the well-known tensile and ligand effects of the substrate in the center over the supported noble metal layer [3]. The objective of the present work is to synthesize, characterize and evaluate electrochemically a platinum and cobalt catalyst supported in Vulcan XC-72R with core-shell structure that shows good activity and stability for the oxygen reduction reaction.

## METHODOLOGY

The synthesis by chemical route of the electrocatalyst of platinum and cobalt were by Polyol method, with sodium borohydride as reducing agent were performed assisted with microwaves. The physical characterization was carried out by X-ray diffraction (XRD), Specific Area (BET), Scanning Electron Microscopy (SEM), Elemental Analysis by X-ray Dispersive Energy (EDAX) and Transmission Electron Microscopy (TEM). The electrochemical evaluation was performed using Cyclic Voltammetry, Linear Voltammetry with rotary ring-disk electrode.

## RESULTS

A carbon-supported PtCo electrocatalyst (20 wt. % loading) was prepared by a two-step microwave-assisted polyol modified method. Ethylene glycol and $NaBH_4$, a strong reducing agent, were utilized. A complex produced by reacting ethylene glycol with sodium borohydride served as a reducing agent and as a stabilizer for preventing the growth of metal particles. First, Co nanoparticles from $CoCl_2$ were reduced by heating with a household microwave oven in several cycles on and off, followed by washing and drying. Secondly, platinum was incorporated onto the cobalt particles with the same method.

## DISCUSSION

A certain proportion of core-shell nanoparticles was obtained, as observed by transmission electronic microscopy and supported by x-ray diffraction. Particle size was in the range of 3-5 nm. The synthesized electrocatalyst showed a good activity for the oxygen reduction reaction (ORR) as well as good stability. Activity was enhanced by the core-shell structure as it causes electronic and ligand effects which accelerate the sluggish kinetics of ORR in fuel cell systems. The use of microwave heating was useful as it induced the synthesis of catalyst nanoparticles in a very short reaction time and with high yield.

## CONCLUSION

A core-shell PtCo electrocatalyst with good activity for the ORR and good stability was successfully prepared by a two-step microwave-assisted polyol modified method. Activity was enhanced by the core-shell structure as it causes electronic and ligand effects which accelerate the sluggish kinetics of oxygen reduction reaction. The use of microwave heating was useful as it induced the synthesis of catalyst with nanometric size in a very short reaction time and with high yield.

**REFERENCES**

[1] K. Kordesch, G. Simader (1996) Fuel cells and their applications. VCH, Weinheim
[2] C. Wang, N.M. Markovic, V.R. Stamenkovic, ACS Catal 2 (2012) 891.
[3] W.Z. Li, Z.W. Chen, L.B. Xu, Y.S. Yan, J Power Sources 195 (2010) 2534.

# Microbial Control Measures for Microwaveable Ready-to-cook and Eat Foods

**P.Michael Davidson**

[2]University of Tennessee, Department of Food Science, Knoxville, TN

## INTRODUCTION

For many years, food processors have marketed food products that are frozen and designed to be heated in microwave ovens prior to consumption. They are primarily intended for consumer convenience. Many of these products contain partially cooked or uncooked foods that require exposure to a minimum temperature and time to eliminate the potential presence of foodborne pathogenic bacteria. Thus, they are actually ready-to-cook and eat foods (RTC) rather than fully cooked "heat and eat" foods. To ensure safety of these products, processors include package instructions for consumers that list minimum temperatures that products should achieve during heating. It is expected that consumers will check the final temperatures of these products using handheld thermometers prior to consumption. Essentially, the consumer becomes the final "critical control point" in a safe process. However, there have been several foodborne illness outbreaks associated with these products indicating that reliance on consumers to follow package instructions is less than totally successful. This, coupled with the desire by consumers and the industry for "clean" labels, increases the risk by eliminating the option for use of synthetic antimicrobial compounds. These compounds potentially could be used alone or in concert with heat to reduce the pathogens. While there are no simple solutions to the elimination of foodborne illness risk with RTC foods, processors have some options to improving the safety of foods that are intended to be cooked in a microwave as a safety step. One option might be the use of naturally occurring antimicrobial compounds which could work concurrently with heat to increase lethality of the heating process. Additionally, newer technologies are available could increase the lethality of processes prior to freezing without detrimentally affecting the quality of the final product. These include microwave pasteurization and high pressure processing. The overall objective of this presentation is to give overviews of the status of the problems associated with RTC foods and some of the potential solutions that could help reduce or eliminate the problems.

# Use of Clean Label Natural Antimicrobials in Food for Assurance of Shelf Life and Food Safety

**Jairus R. D. David**

Conagra Brands, Omaha, Nebraska

**ABSTRACT**

Meeting current consumer demand for clean-label natural ingredients, including antimicrobial preservatives in food is a business imperative. There is a need to consider competing criteria — efficacy in food, sensory impact, cost-in-use, and regulatory compliance — while co-optimizing for sustainable use. The process of adding new, removing, or replacing any existing functional ingredient entails a significant learning curve and investments. Steps for adding or replacing antimicrobials to foods should be done with abundance of caution. Food companies with strong R&D and supporting science and technology will gain a competitive advantage.

**REFERENCES**

[1] David, J.R.D., Steenson, L.R., and Davidson, P.M. 2013. Expectations and Applications of Natural Antimicrobials to Foods: A Guidance Document for the Supplier, User, Research and Development and Regulatory Agencies. Journal of Food Protection Trends, 33 (4): 241 – 250.

[2] Boxman, R., and E. Boxman. 2017. Communicating Science. World Scientific Publishing Co.

# Expert Cooking Intelligence 2017 Update – The Death of the Microwave?

**Steven J. Drucker**

Droaster Laboratories, LLC

Large segments of the frozen microwave food market shrink year over year in unit shipments. Microwave oven feature innovations march in lockstep—with production motivated factories focused on everyday low price, fear of innovation on the part of their customers and brands cut loose from their historic nurturing nests, even while every selling season big retailers beg for something new.

Meanwhile, meals and meal plans proliferate—stretching the boundaries of expert cooking intelligence while most offerings focus on the large numbers that a few percentage points of the market place can deliver.

While demand surges from large numbers of consumers for faster, healthier and better, the microwave faces its own limitations with regards to quality, but remains central for its speed and convenience.

True advances in expert cooking intelligence languish—not for want of effort but because of timidity on the part of appliance industry's hesitation to step out of line.

None of which bodes well for the microwave as we know it.

Q: Is there a 21st- century kitchen that is possibly post microwave? If so—what will it look like for the 99%?

 

# Notes

# Notes

# Notes